Electronic Research Archive

https://www.aimspress.com/journal/era

ERA, 34(2): 1238–1268.
DOI: 10.3934/era.2026057
Received: 09 November 2025
Revised: 19 December 2025
Accepted: 04 January 2026
Published: 06 February 2026

Research article

Local stability and bifurcation of multi-delay fractional-order bidirectional ring neural networks with reaction-diffusion

Yi Min[1,2,*]

[1] College of Mathematics and Physics, China Three Gorges University, Yichang 443002, China

[2] Three Gorges Mathematical Research Center, China Three Gorges University, Yichang 443002, China

* **Correspondence:** Email: miny202511@163.com.

Abstract: This paper investigated the Hopf bifurcation in fractional-order ring neural networks incorporating multiple time delays (leakage, transmission, and distributed delays) and reaction-diffusion effects. By introducing virtual neurons into the original system, a new model capable of equivalently describing the influence of distributed time delays was constructed. The critical conditions for the emergence of pure imaginary roots in the characteristic equation were analytically determined using the Coates flow graph and the holistic element method. Furthermore, by selecting the leakage and transmission delays as bifurcation parameters, explicit criteria for local stability and the existence of Hopf bifurcation were established. The theoretical findings were substantiated through numerical simulations.

Keywords: reaction-diffusion; distributed-time delay; fractional order; Hopf bifurcation

1. Introduction

Nowadays, neural networks have demonstrated extensive application potential in various fields, including medical science [1], deep learning [2], and system evaluation [3]. With the deepening of research, a large number of artificial neural network models have been established, and the rich nonlinear dynamic behaviors of neural networks have been revealed, such as stability, bifurcation, chaos, etc. Among them, Hopf bifurcation, as one of the most representative behaviors in the bifurcation field, has been widely applied in the fields of biology, economics, engineering, etc. [4–6]

In recent years, the rapid development of artificial intelligence has greatly promoted bionics and the research on human brain mechanisms. In the central nervous system, neurons receive and transmit information through dendrites and use synapses to pass it on to other neurons, forming a highly complex network connection structure. The ring structure, as a fundamental topological form of neural networks, has received extensive attention in brain science and related fields.

In 1994, Baldi and Atiya first proposed a class of integer-order neural networks with a unidirectional loop structure composed of n neurons [7]. In 2013, Cai et al. [8] analyzed the influence of the total time delay on a unidirectional loop on the stability of the model and Hopf bifurcation. In 2018, Huang et al. [9] extended this model to a fractional-order form and systematically investigated its bifurcation dynamics. In 2019, Xu et al. [10] further proposed a bidirectional double-ring structure based on the single-ring framework. However, in the real world, there is a widespread phenomenon of two-way information transmission, such as client-server communication architectures, closed-loop feedback in sensor-controller-actuator systems, and reciprocal signaling in neural networks. Inspired by this, researchers introduced the bidirectional transmission mechanism into artificial neural networks to explore their complex dynamic characteristics. In [11, 12], scholars applied the Coates flow graph [13] method to solve the computational problem of high-dimensional feature matrices for bidirectional networks with hyperloop structures and multiple delays. Subsequently, Dai [14] proposed a bidirectional double-loop coupled fractional-order network sharing two nodes and studied the bifurcation dynamics of this network. In [15–17], high-dimensional fractional-order networks with multi-ring shared nodes were investigated, establishing sufficient conditions for stability and Hopf bifurcation induced by time delays.

In the dynamic research of neural networks, the existence of time delays is a key factor inducing complex dynamic behaviors such as oscillations, bifurcations, and chaos. Time delays in real neural networks exhibit multiple types, including leakage delays [18, 19], transmission delays, and distributed delays [20–22]. It is worth noting that Xu et al. [21] effectively simplified the impact of distribution delay in high-dimensional networks by introducing the method of virtual neurons. This train of thought provides an important reference for us on how to reasonably simplify the model and maintain the essential characteristics of dynamics when dealing with complex neural network structures.

These dynamic processes dominated by time delays are often accompanied by memory-dependent characteristics. For example, hippocampal neurons continuously invoke historical information of preceding signals during spatial memory encoding, a feature that can be accurately depicted by fractional-order operators. In real biological neural networks, reaction-diffusion phenomena coexist naturally with the aforementioned characteristics. The conduction of neural signals does not rely solely on direct transmission between synapses, but can also be achieved indirectly through media surrounding neurons, such as cerebrospinal fluid, extracellular fluid, etc.

In 2015, Tian et al. [22] analyzed the Hopf bifurcation of reaction-diffusion neural networks with leakage delays and distributed synaptic transmission delays. Wang et al. [23] investigated synchronous bifurcation and stability in reactive-diffusion ring neurons with time delay. Meanwhile, high-dimensional neural networks have gradually become a research hotspot. In 2022, Chen et al. [24] proposed a class of high-dimensional reaction-diffusion neural networks with multiple delays and conical structures, and studied their stability and Hopf bifurcation. In 2023, He et al. [25] designed a full-dimensional nonlinear state feedback control strategy to optimize the dynamic behavior of multi-delay high-dimensional reaction-diffusion neural networks with binary tree structures. Lu et al. [26] studied a multi-delay high-dimensional reaction-diffusion neural network with bidirectional associative memory, focusing on the influence of network scale and diffusion rate on spatiotemporal dynamics. It should be emphasized that the topological structure of neural networks directly determines the path and efficiency of information transmission. A deep understanding of these topological properties is not only essential for revealing the brain's information processing mechanisms but also provides critical theoretical support for building more efficient and intelligent artificial systems [27–29].

The introduction of fractional-order reaction-diffusion models has provided a new research perspective for this field [20, 30–35] and greatly enriched the dynamic behaviors of the system. Li et al. and Sun et al. [30, 31] investigated the complete synchronization problem of Caputo-type fractional-order reaction-diffusion memristive neural networks with specific discrete constant delays by designing Lyapunov functions. In 2020, Lin et al. [32] mainly studied the Turing patterns of a class of delayed reaction-diffusion neural networks with Caputo-type fractional derivatives. Datsko et al. [33, 34] carried out research on fractional-order reaction-diffusion systems: On the one hand, they analyzed the chaotic dynamic characteristics of the Bonhoeffer–van der Pol fractional-order reaction-diffusion system; on the other hand, they explored the stability of the two-component time-fractional reaction-diffusion system in the linear stage. The results show that when the fractional derivative order takes a specific value, a new type of instability will occur in the system. Hymavathi et al. [20] studied the synchronization problem based on pinning control for fractional-order neural networks with constant delays, distributed delays, and reaction-diffusion terms.

In ecosystems, both predators and prey exhibit synergistic characteristics of fractional order, bidirectional coupling, multiple types of time delays, and reaction-diffusion. Taking the interaction between wolf and deer populations as an example, the number of wolves and deer among populations influence each other, forming a bidirectional coupling relationship; prey disperse and migrate (reaction-diffusion effect); predators require time to digest prey and reproduce (delay mechanism); and populations have long-term memory characteristics in their evolution (fractional-order operator). These elements together determine the complex dynamics such as oscillation and bifurcation of population sizes [36, 37]. Therefore, combining fractional-order operators with multiple types of time delays and reaction-diffusion effects is essentially a synergistic simulation of biological neural networks, which can improve the bionic accuracy of the model. Although existing studies have partially involved elements such as fractional order, time delay, and reaction-diffusion, there are still significant gaps: Most studies do not consider the synergistic impact of bidirectional coupling and distributed delays [24]; some fractional-order reaction-diffusion models do not involve bifurcation analysis of high-dimensional systems [20, 32], or do not clarify the coupling mechanism of multiple delay types [34]. However, research on high-dimensional reaction-diffusion neural networks is still in its infancy, and research results are relatively limited. In particular, research combining specific topological structures with multiple factors such as fractional order operators and distributed delays is still scarce and needs further in-depth exploration.

The main contributions of this study are as follows: (i) A multi-delay fractional-order bidirectional ring neural network based on reaction-diffusion was studied. (ii) The critical conditions for the existence of pure virtual roots in the characteristic equations of the system were determined by using the Coates formula and the holistic element method. (iii) Taking leakage delay and transmission delay as bifurcation parameters, respectively, the local stability of the system and Hopf bifurcation were studied. The correctness and validity of the theoretical analysis results were verified through numerical simulation.

The remainder of this paper is structured as follows: In Section 2, a multi-delay fractional-order bidirectional ring neural network model with reaction-diffusion terms is investigated, and its characteristic equation is derived using the Coates flow graph formula combined with the holistic element method. Section 3 establishes explicit criteria for the local stability and the existence of Hopf bifurcation by selecting the leakage delay and transmission delay as bifurcation parameters. Numerical simulations are provided in Section 4 to validate the correctness of the theoretical analysis. Finally, Section 5 concludes the paper.

In this paper, C^n denotes the space of n-times continuously differentiable functions, and N^+ represents the set of positive integers.

2. Preliminaries

In this section, we first introduce the definition of the Caputo fractional derivative. We then study a class of n-dimensional ring-structured neural networks with multiple time delays and reaction-diffusion terms. Finally, the characteristic equation of the system is derived using the Coates flow graph formula.

Lemma 2.1. *([38], [9] Definition 2) For the function $f(t) \in C^n([t_0, +\infty), R)$, its α-order Caputo fractional derivative is defined as*

$$D^\alpha f(t) = \frac{1}{\Gamma(n-\alpha)} \int_{t_0}^{t} (t-s)^{n-\alpha-1} f^{(n)}(s) ds, \tag{2.1}$$

where $t_0 \le t$, $n-1 < \alpha < n\,(n \in N^+)$ and $\Gamma(\cdot)$ is the Gamma function. Especially, when $0 < \alpha < 1$,

$$D^\alpha f(t) = \frac{1}{\Gamma(1-\alpha)} \int_{t_0}^{t} (t-s)^{-\alpha} f'(s) ds.$$

This paper studies a class of fractional-order reaction-diffusion neural networks with multiple time delays in an n-dimensional setting. The network adopts a bidirectional ring topology, as illustrated in Figure 1.

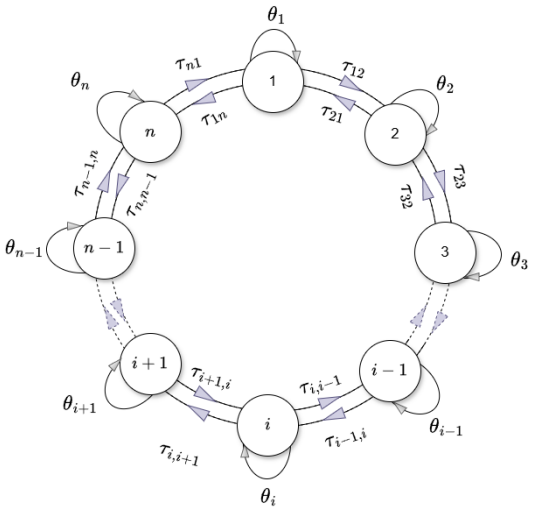

Figure 1. Schematic diagram of the topological structure of a bidirectional ring neural network.

By introducing time delay, distributed time delay, and reaction-diffusion, the spatial dynamics of this

network can be described by the following equations:

$$\begin{cases} D^{\alpha}y_1(x,t) = d_1\Delta y_1(x,t) - a_1' f_{11}\left(y_1(x,t-\theta_1)\right) + b_{21}' f_{21}\left(y_2(x,t-\tau_{21})\right) \\ \qquad +b_{n1}' f_{n1}\left(y_n(x,t-\tau_{n1})\right) + \beta_1 \int_{-\infty}^{t} k(t-s) g_1\left(y_1(x,s)\right) ds, \\ D^{\alpha}y_2(x,t) = d_2\Delta y_2(x,t) - a_2' f_{22}\left(y_2(x,t-\theta_2)\right) + b_{12}' f_{12}\left(y_1(x,t-\tau_{12})\right) \\ \qquad +b_{32}' f_{32}\left(y_3(x,t-\tau_{32})\right) + \beta_2 \int_{-\infty}^{t} k(t-s) g_2\left(y_2(x,s)\right) ds, \\ \qquad \vdots \\ D^{\alpha}y_i(x,t) = d_i\Delta y_i(x,t) - a_i' f_{ii}(y_i(x,t-\theta_i)) + b_{i-1,i}' f_{i-1,i}(y(x,t-\tau_{i-1,i})) \\ \qquad +b_{i+1,i}' f_{i+1,i}(y_{i+1}(x,t-\tau_{i+1,i}) + \beta_i \int_{-\infty}^{t} k(t-s) g_i\left(y_i(x,s)\right) ds, \\ \qquad \vdots \\ D^{\alpha}y_n(x,t) = d_n\Delta y_n(x,t) - a_n' f_{nn}(y_n(x,t-\theta_n)) + b_{1n}' f_{1n}(y_1(x,t-\tau_{1n})) \\ \qquad +b_{n-1,n}' f_{n-1,n}(y(x,t-\tau_{n-1,n})) + \beta_n \int_{-\infty}^{t} k(t-s) g_n\left(y_n(x,s)\right) ds, \end{cases} \tag{2.2}$$

subjecting to Neumann boundary conditions

$$\frac{\partial y_i(x,t)}{\partial v} = 0, i = 1,2,\ldots,n, t > 0, x \in \partial\Omega,$$

with the initial conditions

$$\begin{cases} y_i(x,t) = \phi_i(x,t), i = 1,2,\ldots,n, \\ (x,t) \in [0,\pi] \times [-\max\{\theta_1,\ldots,\theta_n,\tau_{12},\tau_{21},\ldots,\tau_{(n-1)n},\tau_{n(n-1)}\},0], \end{cases}$$

where $i = 1,2,\ldots,n$. Here, $d_i > 0$ denotes the diffusion coefficient, and v is the outward unit normal vector of the smooth boundary $\partial\Omega$. $\Delta = \frac{\partial^2}{\partial x^2}$ is the Laplacian operator in one-dimensional space $\Omega = [0,\pi]$. $y_i(x,t)$ represents the state of the i-th neuron at time t and space x. a_i' and β_i are the self-feedback coefficients of neurons, and $b_{i-1,i}'$ denotes the connection weight from neuron $y_{i-1}(x,t)$ to $y_i(x,t)$. The functions g_i, f_{ii}, and $f_{i-1,i}$ are the activation functions. Furthermore, θ_i denotes the leakage delay of the i-th neuron, which corresponds to the time lag in the decay process of its own state. $\tau_{i-1,i}$ represents the transmission delay between neuron $y_{i-1}(t)$ and neuron $y_i(t)$, accounting for the time consumption in inter-neuronal signal propagation.

The kernel function $k(s)$ is defined on the interval $[0,\infty)$. Commonly used examples include the weak kernel $k(s) = re^{-rs}$ and strong kernel $k(s) = r^2 se^{-rs}$, $r > 0$. This paper focuses on the weak kernel case.

To facilitate the analysis of the system's characteristic equation, we introduce n virtual neurons $u_1(x,t)$, $u_2(x,t)$,$\cdots$, $u_n(x,t)$. The core purpose of introducing these virtual neurons is to convert the distributed delay term $\int_{-\infty}^{t} k(t-s)g_i(y_i(x,s))ds$ in the original system into an equivalent state variable representation, thereby simplifying the model while preserving the essential characteristics of its dynamics. This approach to handling distributed delays can be referred to in [21–23].

The dynamics of these virtual neurons are described as follows:

$$u_i(x,t) = \int_{-\infty}^{t} k(t-s)g_i(y_i(x,s))ds, i = 1,2,\cdots,n.$$

Differentiating both sides of the above equation with respect to time t, we obtain

$$\dot{u}_i(x,t) = \frac{\partial u_i(x,t)}{\partial t} = rg_i(y_i(x,t)) - ru_i(x,t), \quad i = 1,2,\cdots,n.$$

Subsequently, substituting the expression of $u_i(x,t)$ into the original system (2.2), we get

$$\begin{cases} D^\alpha y_1(x,t) = d_1\Delta y_1(x,t) - a_1' f_{11}(y_1(x,t-\theta_1)) + b_{21}' f_{21}(y_2(x,t-\tau_{21})) \\ \qquad +b_{n1}' f_{n1}(y_n(x,t-\tau_{n1})) + \beta_1 u_1(x,t), \\ D^\alpha y_2(x,t) = d_2\Delta y_2(x,t) - a_2' f_{22}(y_2(x,t-\theta_2)) + b_{12}' f_{12}(y_1(x,t-\tau_{12})) \\ \qquad +b_{32}' f_{32}(y_3(x,t-\tau_{32})) + \beta_2 u_2(x,t), \\ \qquad \vdots \\ D^\alpha y_i(x,t) = d_i\Delta y_i(x,t) - a_i' f_{ii}(y_i(x,t-\theta_i)) + b_{i-1,i}' f_{i-1,i}(y(x,t-\tau_{i-1,i})) \\ \qquad +b_{i+1,i}' f_{i+1,i}(y_{i+1}(x,t-\tau_{i+1,i}) + \beta_i u_i(x,t), \\ \qquad \vdots \\ D^\alpha y_n(x,t) = d_n\Delta y_n(x,t) - a_n' f_{nn}(y_n(x,t-\theta_n)) + b_{1n}' f_{1n}(y_1(x,t-\tau_{1n})) \\ \qquad +b_{n-1,n}' f_{n-1,n}(y(x,t-\tau_{n-1,n})) + \beta_n u_n(x,t), \\ \dot{u}_1(x,t) = r g_1(y_1(x,t)) - r u_1(x,t), \\ \qquad \vdots \\ \dot{u}_n(x,t) = r g_n(y_n(x,t)) - r u_n(x,t), \end{cases} \tag{2.3}$$

subjecting to Neumann boundary conditions

$$\begin{cases} \frac{\partial y_i(x,t)}{\partial v} = 0, \\ \frac{\partial u_i(x,t)}{\partial v} = 0, i = 1,2\ldots,n, t > 0, x \in \partial\Omega, \end{cases}$$

with the initial conditions

$$\begin{cases} y_i(x,t) = \phi_i(x,t), \\ u_i(x,t) = \psi_i(x,t), i = 1,2\ldots,n, \\ (x,t) \in [0,\pi] \times [-\max\{\theta_1,\ldots,\theta_n,\tau_{12},\tau_{21},\ldots,\tau_{(n-1)n},\tau_{n(n-1)}\},0], \end{cases}$$

where $\phi, \psi \in C \triangleq C(X, [-\max\{\theta_1,\ldots,\theta_n,\tau_{12},\tau_{21},\ldots,\tau_{(n-1)n},\tau_{n(n-1)}\},0])$, and X is defined by

$$X = \{y_i, u_i \in W^{2,2}(\Omega) | \frac{\partial y_i(x,t)}{\partial v} = \frac{\partial u_i(x,t)}{\partial v} = 0, i = 1,2,\ldots,n, x \in \partial\Omega\}.$$

We assume that

$$\begin{aligned} (H1): & f_{i_1,i_2}, g_i \in \mathbb{C}(R,R), \\ & f_{i_1,i_2}(0) = 0, g_i(0) = 0, \\ & f_{i_1,i_2}'(0) \neq 0, g_i'(0) = 1, i_1 = 1,2\ldots,n, i_2 = 1,2\ldots,n, i = 1,2\ldots,n. \end{aligned}$$

Obviously, the origin $E^* = (0,0,\cdots,0)^T_{1\times 2n}$ is the equilibrium point of (2.3). The linearization of system (2.3) at the origin can be expressed as

$$\begin{cases} D^{\alpha}y_1(x,t) = d_1\Delta y_1(x,t) - a_1y_1(x,t-\theta) + b_{21}y_2(x,t-\tau_{21}) \\ \qquad +b_{n1}y_n(x,t-\tau_{n1}) + \beta u_1(x,t), \\ D^{\alpha}y_2(x,t) = d_2\Delta y_2(x,t) - a_2y_2(x,t-\theta) + b_{12}y_1(x,t-\tau_{12}) \\ \qquad +b_{32}y_3(x,t-\tau_{32}) + \beta u_2(x,t), \\ \qquad \vdots \\ D^{\alpha}y_i(x,t) = d_i\Delta y_i(x,t) - a_iy_i(x,t-\theta) + b_{i-1,i}y_{i-1}(x,t-\tau_{i-1,i}) \\ \qquad +b_{i+1,i}y_{i+1}(x,t-\tau_{i+1,i}) + \beta u_i(x,t), \\ \qquad \vdots \\ D^{\alpha}y_n(x,t) = d_n\Delta y_n(x,t) - a_ny_n(x,t-\theta) + b_{1n}y_1(x,t-\tau_{1n}) \\ \qquad +b_{n-1,n}y(x,t-\tau_{n-1,n}) + \beta u_n(x,t), \\ \dot{u}_1(x,t) = ry_1(x,t) - ru_1(x,t), \\ \qquad \vdots \\ \dot{u}_n(x,t) = ry_n(x,t) - ru_n(x,t), \end{cases} \tag{2.4}$$

where $a_i = a_i' f_{ii}(0),\ b_{n1} = b_{n1}' f_{n1}(0),\ b_{21} = b_{21}' f_{21}(0),\ b_{n-1,n} = b_{n-1,n}' f_{n-1,n}(0),\ b_{1n} = b_{1n}' f_{1n}(0),\ b_{j-1,j} = b_{j-1,j}' f_{j-1,j}(0),\ b_{j+1,j} = b_{j+1,j}' f_{j+1,j}(0)$, and $j = 1, 2, \dots n$.
We assume that

$$\begin{aligned} &(H2): d_i = d,\ a_i = a,\ \beta_i = \beta,\ i = 1, 2, \dots n, \\ &(H3): \theta_1 = \theta_2 = \cdots = \theta_{n-1} = \theta_n = \theta, \\ &\qquad \tau_{12} + \tau_{21} = \tau_{23} + \tau_{32} = \cdots = \tau_{n1} + \tau_{1n} = 2\tau, \\ &\qquad \tau_{12} + \tau_{23} + \cdots + \tau_{n-1,1} + \tau_{n1} = \tau_{1n} + \tau_{n,n-1} + \cdots + \tau_{32} + \tau_{21} = n\tau. \end{aligned}$$

The eigenvalue of Δ in Ω under Neumann boundary conditions is $-k^2$ for $k \in N := \{0, 1, 2, \cdots\}$. The corresponding eigenfunctions are given by

$$\mu_k^1(x) = (\gamma_k, 0, \dots, 0)^T, \mu_k^2(x) = (0, \gamma_k, \dots, 0)^T, \dots, \mu_k^{2n}(x) = (0, 0, \dots, \gamma_k)^T,$$

where $\gamma_k = \frac{\cos(kx)}{\|\cos(kx)\|}$. The set $\{\mu_k^1, \mu_k^2, \dots, \mu_k^{2n}\}_{k=0}^{+\infty}$ constructs a basis of the phase X.

Consequently, the perturbation solution of system (2.4) can be expanded in x as the following Fourier series:

$$(y_1, \dots, y_n, u_1, \dots, u_n)^T = \sum_{k=0}^{\infty} \left(M_k^1, M_k^2, \dots, M_k^{2n}\right)^T e^{\lambda t} \cos kx, \tag{2.5}$$

where $k \in N$ represents the number of waves in space and λ describes the growth rate of the disturbance in time t.

Applying the Laplace transform to system (2.4) and incorporating the Fourier expansion (2.5) leads to the frequency-domain formulation

$$\left(\lambda^{\alpha} + dk^2 + ae^{-\lambda\theta}\right) Y_i(\lambda) = b_{i-1,i}e^{-\lambda\tau_{i-1,i}} Y_{i-1,i}(\lambda) + b_{i+1,i}e^{-\lambda\tau_{i+1,i}} Y_{i+1,i}(\lambda) + \beta U_i(\lambda), \tag{2.6}$$

$$U_i(\lambda) = \frac{r}{\lambda + r} Y_i(\lambda), i = 1, \ldots, n, \tag{2.7}$$

where $Y_i(\lambda)$ and $U_i(\lambda)$ are the Laplace transforms of $y(t)$ and $u(t)$.
Substituting Eq (2.7) into (2.6) eliminates $U_i(\lambda)$, and we get

$$\left(\lambda^\alpha + dk^2 + ae^{-\lambda\theta} - \frac{r\beta}{\lambda + r}\right) Y_i(\lambda) = b_{i-1,i} e^{-\lambda\tau_{i-1,i}} Y_{i-1,i}(\lambda) + b_{i+1,i} e^{-\lambda\tau_{i+1,i}} Y_{i+1,i}(\lambda).$$

Consequently, the dynamics of the entire network are governed by a linear system in the vector $Y(\lambda) = (Y_1(\lambda), \ldots, Y_n(\lambda))$, from which the characteristic matrix $V(\lambda, k)$ of the system at the equilibrium E^* can be directly constructed.

$$V(\lambda, k) = \begin{bmatrix} E(\lambda,k) & -b_{21}e^{-\lambda\tau_{21}} & 0 & \cdots & 0 & -b_{n1}e^{-\lambda\tau_{n1}} \\ -b_{12}e^{-\lambda\tau_{12}} & E(\lambda,k) & -b_{32}e^{-\lambda\tau_{32}} & \cdots & 0 & 0 \\ \vdots & \vdots & \vdots & \ddots & \vdots & \vdots \\ -b_{1n}e^{-\lambda\tau_{1n}} & 0 & 0 & \cdots & -b_{n-1,n}e^{-\lambda\tau_{n-1,n}} & E(\lambda,k) \end{bmatrix},$$

where $E(\lambda, k) = \lambda^\alpha + ae^{-\lambda\theta} + dk^2 - \frac{r\beta}{\lambda+r}$.
The characteristic equation is then given by

$$det(V(\lambda, k)) = 0. \tag{2.8}$$

Lemma 2.2. *([13], Theorem 1) The determinant V of system (2.4) can be calculated by its flow graph G according to the following formula:*

$$detV = (-1)^n \sum_{i=1}^{\rho} (-1)^{n_i} M_i, \tag{2.9}$$

where n is the order of the determinant. ρ represents the number of subgraphs G_i (G_i is a subgraph of G), which is composed of simple disjoint link points. n_i is the number of directed cycles in the subgraph G_i. M_i is the connection gain of the subgraph G_i.

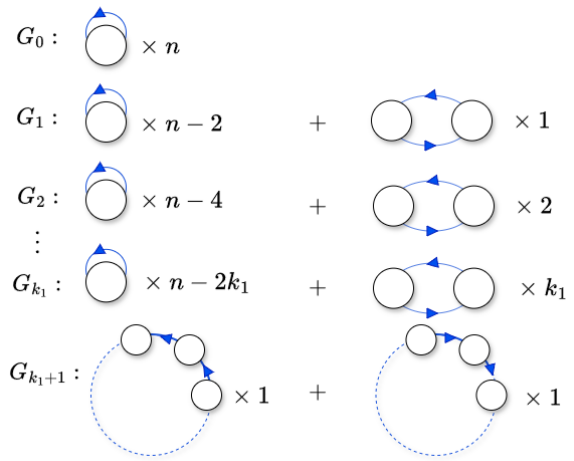

Figure 2. Flow graph decomposition of matrix $V(\lambda, k)$.

The subgraph of the flow graph G of the determinant $V(\lambda, k)$ is shown in Figure 2. Define $c_1 = b_{12}b_{21}$, $c_2 = b_{23}b_{32}$, $c_j = b_{j-1,j}b_{j,j-1}$, and $c_n = b_{n1}b_{1n}$, with $j = 2, 3, \cdots, n-1$. We can use (2.9) to calculate the expression of $detV(\lambda, k)$. As can be easily seen from Figure 2, all subgraphs of the flow graph G can be divided into $k_1 + 2$ non–contact loops, where $k_1 = \lfloor \frac{n}{2} \rfloor$ ($\lfloor \cdot \rfloor$ indicates rounding down).

$$
\begin{aligned}
&G_0 = (-1)^n(\lambda^\alpha + ae^{-\lambda\theta} + dk^2 - \frac{r\beta}{\lambda + r})^n,\\
&G_1 = (-1)^{n-1}(\lambda^\alpha + ae^{-\lambda\theta} + dk^2 - \frac{r\beta}{\lambda + r})^{n-2}\varphi_1 e^{-2\lambda\tau},\\
&G_2 = (-1)^{n-2}(\lambda^\alpha + ae^{-\lambda\theta} + dk^2 - \frac{r\beta}{\lambda + r})^{n-4}\varphi_2 e^{-4\lambda\tau},\\
&\vdots\\
&G_m = (-1)^{n-m}(\lambda^\alpha + ae^{-\lambda\theta} + dk^2 - \frac{r\beta}{\lambda + r})^{n-2m}\varphi_m e^{-2m\lambda\tau},\\
&\vdots\\
&G_{k_1+1} = -\varphi_{k_1+1}e^{-n\lambda\tau},
\end{aligned}
$$

where

$$
\begin{aligned}
&\varphi_1 = \sum_{i=1}^{n} c_i,\\
&\varphi_2 = \sum_{i_1=3}^{n-1} c_1 c_{i_1} + \sum_{i_1=2}^{n-2}\sum_{i_2=i_1+2}^{n} c_{i_1}c_{i_2},\\
&\varphi_m = \sum_{i_1=3}^{n+3-2m}\sum_{i_2=i_1+2}^{n+5-2m}\cdots\sum_{i_{m-1}=i_{m-2}+2}^{n-1} c_1 c_{i_1}c_{i_2}\cdots c_{i_{m-1}} + \sum_{i_1=2}^{n+2-2m}\sum_{i_2=i_1+2}^{n+4-2m}\cdots\sum_{i_i=i_{m-1}+2}^{n} c_{i_1}c_{i_2}\cdots c_{i_m},\\
&\vdots\\
&\varphi_{k_1+1} = b_{12}b_{23}\cdots b_{(n-1)1}b_{n1} + b_{1n}b_{n(n-1)}\cdots b_{32}b_{21}.
\end{aligned}
$$

Finally, we can obtain the characteristic equation of system (2.4)

$$
\begin{aligned}
&(\lambda^\alpha + ae^{-\lambda\theta} + dk^2 - \frac{r\beta}{\lambda + r})^n + \sum_{i=1}^{k_1}(-1)^i(\lambda^\alpha + ae^{-\lambda\theta} + dk^2 - \frac{r\beta}{\lambda + r})^{n-2i}\varphi_i e^{-2i\lambda\tau}\\
&+ (-1)^{n+1}\varphi_{k_1+1}e^{-n\lambda\tau} = 0.
\end{aligned}
\tag{2.10}
$$

Multiply both sides of the equation by $e^{n\lambda\tau}$ and define a holistic element

$$
s(k) = (\lambda^\alpha + ae^{-\lambda\theta} + dk^2 - \frac{r\beta}{\lambda + r})e^{\lambda\tau}.
$$

After substitution, Eq (2.10) becomes

$$
\Phi(s) = s^n(k) + \sum_{i=1}^{k_1}(-1)^i\varphi_i s^{n-2i}(k) + (-1)^{n+1}\varphi_{k_1+1}. \tag{2.11}
$$

We know that there are n roots in Eq (2.11), denoted as $s_j = \xi_j + i\eta_j$, $j = 1, \cdots, n$. This indicates that

$$(\lambda^\alpha + ae^{-\lambda\theta} + dk^2 - \frac{r\beta}{\lambda + r})e^{\lambda\tau} = \xi_j + i\eta_j. \tag{2.12}$$

Remark 2.1. *The characteristic matrix $V(\lambda, k)$ and the corresponding characteristic equation are derived by using the Coates formula, which constructs a key mathematical tool for the dynamic analysis of fractional-order delay ring neural networks. In the matrix structure, the main diagonal elements characterize the self-feedback of individual neurons (including fractional order, time delay, and diffusion effects), while the non-diagonal elements describe the coupled time delay effects between neurons. The ring graph drawn based on this matrix is the same as that in Figure 1. Through flow graph decomposition (Figure 2) and Lemma 2.2, the characteristic equation corresponding to the derivative characteristic matrix $V(\lambda, k)$ can be derived.*

Remark 2.2. *The incorporation of reaction-diffusion terms leads to a characteristic equation (2.10) composed of an infinite set of higher-order transcendental equations parameterized by the wavenumber k. This structure poses a significant challenge for conventional analytical methods. Fortunately, the Coates flow graph formula offers an effective graphical approach to compute the determinant of the characteristic matrix $V(\lambda, k)$ and thus tackles this complex characteristic problem.*

3. Local stability and Hopf bifuraction

Next, we will discuss the stability of model (2.4) and the Hopf bifurcation by analyzing the zero-point distribution of Eq (2.10).

3.1. Case without time delay ($\theta = \tau = 0$)

When $\theta = \tau = 0$, the characteristic equation (2.10) reduces to

$$(\lambda^\alpha + a + dk^2 - \frac{r\beta}{\lambda + r})^n + \sum_{i=1}^{k_1}(-1)^i(\lambda^\alpha + a + dk^2 - \frac{r\beta}{\lambda + r})^{n-2i}\varphi_i + (-1)^{n+1}\varphi_{k_1+1} = 0,$$

where

$$\lambda^\alpha + a + dk^2 - \frac{r\beta}{\lambda + r} = \xi_j + i\eta_j. \tag{3.1}$$

Lemma 3.1. *For $\theta = \tau = 0$, the trivial equilibrium point of network (2.4) is local asymptotic stability if the following condition holds:*
$(H4):\ \xi_j - a < 0, \beta \le 0, j = 1, 2, \ldots, n.$

Proof. Assume Eq (3.1) has a solution satisfying $Re(\lambda) \ge 0$, which implies $|arg(\lambda)| \le \frac{\pi}{2}$. The argument of λ^α is then given by $arg(\lambda^\alpha)$. Accordingly, we obtain $|arg(\lambda^\alpha)| \le \frac{\alpha\pi}{2}$. Since $\alpha \in (0, 1)$, it follows that $\frac{\alpha\pi}{2} < \frac{\pi}{2}$.

By transforming Eq (3.1), we obtain the following expression:

$$\lambda^\alpha - \frac{r\beta(\overline{\lambda} + r)}{(\lambda + r)(\overline{\lambda} + r)} = \xi_j - a - dk^2 + i\eta_j.$$

From this result, we obtain the following expressions:

$$Re(\lambda^\alpha) = \frac{(\xi_j - a - dk^2)[(Re(\lambda) + r)^2 + (Im(\lambda))^2] + r\beta(Re(\lambda) + r)}{[Re(\lambda) + r]^2 + [Im(\lambda)]^2}.$$

Given that $[Re(\lambda) + r]^2 + [Im(\lambda)]^2 > 0, Re(\lambda) > 0, r > 0, \xi_j - a - dk^2 < 0$, and $\beta \leq 0$, it can be deduced that $Re(\lambda^\alpha) < 0$. This result contradicts the condition $Re(\lambda^\alpha) > 0$. It follows that all characteristic roots of Eq (3.1) have negative real parts. □

Remark 3.1. *The characteristic equation (3.1) can be simplified to a fractional polynomial* $\lambda^{1+\alpha} + a\lambda + b\lambda^\alpha + c = 0$ *in the following form. Among them, the coefficients a, b, and c are all functions of the wavenumber k. The stability problem of such polynomial equations can be analyzed by referring to the method proposed in [39]. This method provides a set of approaches for handling the root distribution of such characteristic equations. Based on this train of thought, this paper deduces Lemma 3.1 and establishes sufficient conditions to ensure that all roots of Eq (3.1) lie in the left semi-complex plane.*

3.2. Selecting τ as the bifurcation parameter

When $\tau = 0$, Eq (2.12) can be transformed into

$$J_1 e^{-\lambda\theta} + J_2 = 0, \tag{3.2}$$

where

$$\begin{aligned} J_1 &= a(\lambda + r), \\ J_2 &= (\lambda^\alpha + dk^2 - \xi_j - i\eta_j)(\lambda + r) - r\beta. \end{aligned}$$

For simplicity, the real and imaginary parts of $J_l(\lambda)$ $(l = 1, 2)$ can be expressed as J_l^R, J_l^I, respectively. Let $\lambda = i\omega$ $(\omega > 0)$ be a pure imaginary root of Eq (3.2), and we can obtain

$$\begin{cases} J_1^R \cos\omega\theta + J_1^I \sin\omega\theta = -J_2^R, \\ J_1^I \cos\omega\theta - J_1^R \sin\omega\theta = -J_2^I, \end{cases} \tag{3.3}$$

where

$$\begin{aligned} J_1^R &= ar, \\ J_1^I &= a\omega, \\ J_2^R &= r\left(\omega^\alpha \cos\frac{\alpha\pi}{2} + dk^2 - \xi_j\right) - \omega\left(\omega^\alpha \sin\frac{\alpha\pi}{2} - \eta_j\right) - r\beta, \\ J_2^I &= \omega\left(\omega^\alpha \cos\frac{\alpha\pi}{2} + dk^2 - \xi_j\right) + r\left(\omega^\alpha \sin\frac{\alpha\pi}{2} - \eta_j\right). \end{aligned}$$

From (3.3), we acquire

$$\begin{cases} \cos\omega\theta = \frac{-J_1^R \cdot J_2^R - J_1^I \cdot J_2^I}{(J_1^R)^2 + (J_1^I)^2} = B_1(\omega), \\ \sin\omega\theta = \frac{-J_1^I \cdot J_2^R + J_1^R \cdot J_2^I}{(J_1^R)^2 + (J_1^I)^2} = B_2(\omega). \end{cases} \tag{3.4}$$

It can obviously be concluded from equation system (3.4) that

$$(B_1(\omega))^2 + (B_2(\omega))^2 = \frac{\left(J_2^R\right)^2 + \left(J_2^I\right)^2}{\left(J_1^R\right)^2 + \left(J_1^I\right)^2} = 1. \tag{3.5}$$

We construct a function $\Psi_k(\omega)$ on $(0, +\infty)$ from Eq (3.5) such that the existence of its zeros directly determines the solvability of the equation. Specifically, Eq (3.5) admits a solution if and only if $\Psi_k(\omega)$ possesses at least one positive zero.

$$\begin{aligned}\Psi_k(\omega) =&\omega^{2\alpha+2} + 2\omega^{\alpha+2}\left(\cos\frac{\alpha\pi}{2}dk^2 - \cos\frac{\alpha\pi}{2}\xi_j - \sin\frac{\alpha\pi}{2}\eta_j\right) + \omega^2\left(\left(dk^2 - \xi_j\right)^2 + \eta_j^2\right.\\ &\left. - a^2\right) + 2\omega^{\alpha+1}r\beta\sin\frac{\alpha\pi}{2} + \omega^{2\alpha}r^2 - 2\omega r\beta\eta_j + 2r^2\omega^{\alpha}\left(\cos\frac{\alpha\pi}{2}dk^2 - \cos\frac{\alpha\pi}{2}\xi_j\right.\\ &\left. - \sin\frac{\alpha\pi}{2}\eta_j - \beta\cos\frac{\alpha\pi}{2}\right) + r^2\left(\left(dk^2 - \xi_j - \beta\right)^2 + \eta_j^2 - 4\beta\xi_j - a^2\right).\end{aligned} \tag{3.6}$$

Lemma 3.2. *Define the root of Eq (2.11) as s_j. The following results apply characteristic equation (2.10):*

i) If there exists some $j \in \{1, 2, \ldots, n\}$ such that the following condition holds:
$(H5): \ (\xi_j + \beta)^2 < a^2 + 4\beta\xi_j - \eta_j^2$,
then, for this specific j, the function (3.6) has at least one zero point for every $k \in \{0, 1, 2, \ldots, k_T\}$ (where k_T is a finite non-negative integer). Correspondingly, Eq (3.5) has at least one positive real root, and as a consequence, the characteristic equation (2.10) admits at least one pair of pure imaginary roots.

ii) For every $j \in \{1, 2, \ldots, n\}$, there exists a sufficiently large $K_j \in N$ such that the following conditions hold for all $k \geqslant K_j$:
$(H6): \ \cos\frac{\alpha\pi}{2}dk^2 - \cos\frac{\alpha\pi}{2}\xi_j - \sin\frac{\alpha\pi}{2}\eta_j > 0$,
$(H7): \ \left(dk^2 - \xi_j - \beta\right)^2 + \eta_j^2 - \beta^2 - a^2 - 4\beta\xi_j > 0$,
$(H8): \ \left(dk^2 - \xi_j\right)^2 - a^2 - \beta^2\sin^2\frac{\alpha\pi}{2} > 0$.
Under these conditions, the function $\Psi_k(\omega) > 0$ holds for all $\omega > 0$. This implies that Eq (3.5) has no positive real roots. And since k is a parameter in the characteristic equation (2.10), this further means that no solutions exist for (2.10) corresponding to $k \geqslant K_j$. Thus, the number of valid k-values for (2.10) is restricted.

Proof. (i) If $(\xi_j + \beta)^2 < a^2 + 4\beta\xi_j - \eta_j^2$ for some $j \in \{1, 2, \ldots, n\}$ is established, it will exist for a particular $k_t > 0$, making $(dk_t^2 - \xi_j - \beta)^2 + \eta_j^2 - 4\beta\xi_j - a^2 = 0$.
Solving for k_t, we obtain:

$$k_t = \sqrt{\frac{\sqrt{a^2 + 4\beta\xi_j - \eta_j^2} + \xi_j + \beta}{d}}.$$

We further define k_t to satisfy the range $k_T < k_t \leq k_T + 1$ where $k_T \in N$.
When $k = 0, 1, 2, \ldots, k_T$, we have

$$\Psi_k(0) = r^2\left((dk^2 - \xi_j - \beta)^2 + \eta_j^2 - 4\beta\xi_j - a^2\right) < 0,$$

and $\lim\limits_{\omega\to+\infty}\Psi_k(\omega) = +\infty$. According to the zero point theorem, Eq (3.5) must have a positive root, that is, Eq (2.10) has a pair of pure imaginary roots.

(ii) To prove (ii), we transform Eq (3.6) into the following equivalent form:

$$\begin{aligned}\Psi(\omega) =&\omega^{2\alpha+2} + 2\omega^{\alpha+2}\left(\cos\frac{\alpha\pi}{2}dk^2 - \cos\frac{\alpha\pi}{2}\xi_j - \sin\frac{\alpha\pi}{2}\eta_j\right)\\ &+ \omega^2\left(\left(dk^2-\xi_j\right)^2 - a^2 - \beta^2\sin^2\frac{\alpha\pi}{2}\right) + \left(\omega^2\beta^2\sin^2\frac{\alpha\pi}{2} + 2\omega^{\alpha+1}r\beta\sin\frac{\alpha\pi}{2} + \omega^{2\alpha}\cdot r^2\right)\\ &+ \left(\omega^2\eta_j^2 - 2\omega r\beta\eta_j + r^2\beta^2\right) + 2r^2\omega^{\alpha}\left(\cos\frac{\alpha\pi}{2}dk^2 - \cos\frac{\alpha\pi}{2}\xi_j - \sin\frac{\alpha\pi}{2}\eta_j - \beta\cos\frac{\alpha\pi}{2}\right)\\ &+ r^2\left(\left(dk^2-\xi_j-\beta\right)^2 + \eta_j^2 - \beta^2 - 4\beta\xi_j - a^2\right)\\ =&\omega^{2\alpha+2} + 2\omega^{\alpha+2}\left(\cos\frac{\alpha\pi}{2}dk^2 - \cos\frac{\alpha\pi}{2}\xi_j - \sin\frac{\alpha\pi}{2}\eta_j\right)\\ &+ \omega^2\left(\left(dk^2-\xi_j\right)^2 - a^2 - \beta^2\sin^2\frac{\alpha\pi}{2}\right) + \left(\omega\beta\sin\frac{\alpha\pi}{2} + \omega^{\alpha}r\right)^2\\ &+ \left(\omega\eta_j - r\beta\right)^2 + 2r^2\omega^{\alpha}\left(\cos\frac{\alpha\pi}{2}dk^2 - \cos\frac{\alpha\pi}{2}\xi_j - \sin\frac{\alpha\pi}{2}\eta_j - \beta\cos\frac{\alpha\pi}{2}\right)\\ &+ r^2\left(\left(dk^2-\xi_j-\beta\right)^2 + \eta_j^2 - \beta^2 - 4\beta\xi_j - a^2\right).\end{aligned}$$

For $\omega > 0$, the terms $\omega^{2\alpha+2}$, $(\omega\beta\sin\frac{\alpha\pi}{2} + \omega^{\alpha}r)^2$, and $(\omega\eta_j - r\beta)^2$ are inherently positive. Therefore, a sufficient condition for $\Psi_k(\omega) > 0$ is that the coefficients of the $\omega^{\alpha+2}$, ω^2, and ω^{α} terms, along with the constant term, are all positive. Furthermore, there exists a minimal $K_j \in N$ satisfying conditions $(H6)$–$(H8)$. Consequently, for all $k \geqslant K_j$, we have $\Psi_k(\omega) > 0$, which implies that Eq (3.5) admits no solution.

□

Let the zero solution of function (3.6) have m_{jk} solutions for each j and the corresponding k, and this solution is defined as $\omega_{m_{jk}}$.

$$\theta_{m_{jk}}^{(l)} = \frac{1}{\omega_{m_{jk}}}[\arccos B_1(\omega_{m_{jk}}) + 2l\pi], l = 0, 1, \ldots, j = 1, 2, \ldots, n, k = 0, 1, \ldots, K_j, \tag{3.7}$$

$$\theta_0 = \theta_{m_{j_0k_0}}^{(0)} = \min_{\substack{j=1,2,\ldots,n\\ k=0,1,\ldots,K_j}}\{\theta_{m_{jk}}^{(0)}\}, \omega_0 = \omega_{m_{j_0k_0}}. \tag{3.8}$$

Remark 3.2. *Lemma 3.2 (ii) establishes that the existence of a solution ω to Eq (3.5) depends critically on the wavenumber k. It rigorously guarantees that for all wavenumbers k exceeding a certain critical threshold K_j, such solutions ω cease to exist.*

When $\theta \in [0, \theta_0)$, $\tau > 0$, Eq (2.12) can be transformed into

$$K_1 e^{\lambda\tau} + K_2 = 0, \tag{3.9}$$

$$K_1 = (\lambda^{\alpha} + ae^{-\lambda\theta} + dk^2)(\lambda + r) - r\beta,$$

$$K_2 = (-\xi_j - i\eta_j)(\lambda + r).$$

For simplicity, the real and imaginary parts of $K_l(\lambda)$ $(l = 1, 2)$ can be expressed as K_l^R, K_l^I, respectively. Let $\lambda = i\omega$ $(\omega > 0)$ be a pure imaginary root of Eq (3.9), and we can obtain

$$\begin{cases} K_1^R \cos\omega\tau - K_1^I \sin\omega\tau = -K_2^R, \\ K_1^I \cos\omega\tau + K_1^R \sin\omega\tau = -K_2^I, \end{cases} \tag{3.10}$$

where

$$\begin{aligned} K_1^R &= -\omega^{\alpha+1}\sin\frac{\alpha\pi}{2} + a\omega\sin\omega\theta + r\omega^{\alpha}\cos\frac{\alpha\pi}{2} + ar\cos\omega\theta + rdk^2 - r\beta, \\ K_1^I &= \omega^{\alpha+1}\cos\frac{\alpha\pi}{2} + a\omega\cos\omega\theta + \omega dk^2 + r\omega^{\alpha}\sin\frac{\alpha\pi}{2} - ar\sin\omega\theta, \\ K_2^R &= \eta_j\omega - r\xi_j, \\ K_2^I &= -\xi_j\omega - r\eta_j. \end{aligned}$$

From (3.10), we acquire

$$\begin{cases} \cos\omega\tau = \frac{-K_1^R\cdot K_2^R - K_1^I\cdot K_2^I}{(K_1^R)^2+(K_1^I)^2} = A_1(\omega), \\ \sin\omega\tau = \frac{K_1^I\cdot K_2^R - K_1^R\cdot K_2^I}{(K_1^R)^2+(K_1^I)^2} = A_2(\omega). \end{cases} \tag{3.11}$$

It can obviously be concluded from equation system (3.11) that

$$(A_1(\omega))^2 + (A_2(\omega))^2 = \frac{(K_2^R)^2 + (K_2^I)^2}{(K_1^R)^2 + (K_1^I)^2} = 1. \tag{3.12}$$

We construct a function $\hat{\Psi}_k(\omega)$ on $(0, +\infty)$ from Eq (3.12), such that the existence of its zeros directly determines the solvability of the equation. Specifically, Eq (3.12) admits a solution if and only if $\hat{\Psi}_k(\omega)$ possesses at least one positive zero.

$$\begin{aligned} \hat{\Psi}_k(\omega) =& \omega^{2\alpha+2} + 2a\omega^{\alpha+2}\cos\left(\frac{\alpha\pi}{2} + \omega\theta\right) + 2dk^2\cos\frac{\alpha\pi}{2}\omega^{\alpha+2} + 2dk^2a\cdot\omega^2\cos\omega\theta \\ &+ \left(\left(dk^2\right)^2 + a^2 - \left(\xi_j^2 + \eta_j^2\right)\right)\omega^2 + r^2\omega^{2\alpha} + 2ar^2\omega^{\alpha}\cos\left(\frac{\alpha\pi}{2} + \omega\theta\right) \\ &+ 2r^2\cos\frac{\alpha\pi}{2}\left(dk^2 - \beta\right)\omega^{\alpha} + 2r\beta\sin\frac{\alpha\pi}{2}\omega^{\alpha+1} + 2r^2\left(adk^2 - a\beta\right)\cos\omega\theta \\ &- 2ar\beta\omega\sin\omega\theta + r^2\left(\left(dk^2\right)^2 + a^2 - 2\beta dk^2 + \beta^2 - \xi_j^2 - \eta_j^2\right). \end{aligned} \tag{3.13}$$

Lemma 3.3. *Define the root of Eq (2.11) as s_j. The following results apply characteristic equation (2.10):*

i) If there exists some $j \in \{1, 2, \ldots, n\}$ such that the following condition holds:
$(H9)$: $(a - \beta)^2 < \xi_j^2 + \eta_j^2$,
then, for this specific j, the function (3.13) has at least one zero point for every $k \in \{0, 1, 2, ..., \hat{k}_T\}$. Correspondingly, Eq (3.12) has at least one positive real root, and as a consequence, the characteristic equation (2.10) admits at least one pair of pure imaginary roots.

ii) For every $j \in \{1, 2, \ldots, n\}$, there exists a sufficiently large $\hat{K}_j \in N$ such that the following conditions hold for all $k \geqslant \hat{K}_j$:
$(H10): \ dk^2 \cos\frac{\alpha\pi}{2} - |a| > 0,$
$(H11): \ \left(dk^2\right)^2 - 2dk^2|a| - \xi_j^2 - \eta_j^2 > 0,$
$(H12): \ \left(dk^2\right)^2 - 2|a|dk^2 - \xi_j^2 - \eta_j^2 + a^2 - 2\beta dk^2 + 2|a|\beta - \beta^2 \sin^2\frac{\alpha\pi}{2} > 0.$
Under these conditions, the function $\hat{\Psi}_k(\omega) > 0$ holds for all $\omega > 0$. This implies that Eq (3.12) has no positive real roots. And since k is a parameter in the characteristic equation (2.10), this further means that no solutions exist for (2.10) corresponding to $k \geqslant \hat{K}_j$.

Proof. (i) If $(a-\beta)^2 < \xi_j^2 + \eta_j^2$ for some $j \in \{1, 2, \ldots, n\}$ is established, it will exist for a particular $\hat{k}_t > 0$, making $(dk^2 + a - \beta)^2 - \xi_j^2 - \eta_j^2 = 0$.
Solving for $\hat{k}_t$, we obtain:

$$\hat{k}_t = \sqrt{\frac{\sqrt{\xi_j^2 + \eta_j^2} + \beta - a}{d}}.$$

We further define $\hat{k}_t$ to satisfy the range $\hat{k}_T < \hat{k}_t \leq \hat{k}_T + 1$ where $\hat{k}_T \in N$.
When $k = 0, 1, 2, \ldots, \hat{k}_T$, we have

$$\hat{\Psi}_k(0) = r^2\left((dk^2 + a - \beta)^2 - \xi_j^2 - \eta_j^2\right) < 0,$$

and $\lim\limits_{\omega \to +\infty} \hat{\Psi}_k(\omega) = +\infty$. According to the zero point theorem, (3.12) must have a positive root, that is, Eq (2.10) has a pair of pure imaginary roots.

(ii) By leveraging the bounds $\cos(\cdot) \geq -1$ and $\sin(\cdot) \geq -1$ to relax the trigonometric terms in $\hat{\Psi}_k(\omega)$, we construct a function $\hat{g}_k(\omega)$ such that $\hat{\Psi}_k(\omega) \geq \hat{g}_k(\omega)$ holds.

$$\begin{aligned}\hat{g}_k(\omega) =& \omega^{2\alpha+2} + \left(2dk^2\cos\frac{\alpha\pi}{2} - 2|a|\right)\omega^{\alpha+2} + \left(\left(dk^2\right)^2 - 2dk^2|a| + a^2 - \xi_j^2 - \eta_j^2\right)\omega^2 \\ &+ 2r\beta\sin\frac{\alpha\pi}{2}\omega^{\alpha+1} + r^2\omega^{2\alpha} + 2r^2\left(\cos\frac{\alpha\pi}{2}\left(dk^2 - \beta\right) - |a|\right)\omega^{\alpha} \\ &+ 2|a|r\beta\omega + r^2\left(\left(dk^2\right)^2 + a^2 - 2\beta dk^2 + \beta^2 - \xi_j^2 - \eta_j^2 - 2|a|\left(dk^2 - \beta\right)\right).\end{aligned}$$

The presence of negative coefficients in the terms $2r\beta\sin\frac{\alpha\pi}{2}\omega^{\alpha+1}$ and $2|a|r\beta\omega$ of $\hat{g}(\omega)$ is handled by completing the square. We reformulate the relevant parts of $\hat{g}(\omega)$ into the squares $\left(\omega^{\alpha+1} + r\beta\sin\frac{\alpha\pi}{2}\right)^2$ and $(|a|\omega + r\beta)^2$, which are guaranteed to be non–negative for all $\omega > 0$.

$$\begin{aligned}\hat{g}_k(\omega) =& \left(\omega^{\alpha+1} + r\beta\sin\frac{\alpha\pi}{2}\right)^2 + \left(2dk^2\cos\frac{\alpha\pi}{2} - 2|a|\right)\omega^{\alpha+2} + r^2\omega^{2\alpha} \\ &+ \left(\left(dk^2\right)^2 - 2dk^2|a| - \xi_j^2 - \eta_j^2\right)\omega^2 + 2r^2\left(\cos\frac{\alpha\pi}{2}\left(dk^2 - \beta\right) - |a|\right)\omega^{\alpha} + (|a|\omega + r\beta)^2 \\ &+ r^2\left(\left(dk^2\right)^2 - 2|a|dk^2 + a^2 - \xi_j^2 - \eta_j^2 - 2\beta dk^2 + 2|a|\beta - \beta^2\sin^2\frac{\alpha\pi}{2}\right).\end{aligned}$$

Given that $\omega > 0$, the terms $\left(\omega^{\alpha+1} + r\beta\sin\frac{\alpha\pi}{2}\right)^2$, $r^2\omega^{2\alpha}$, and $(|a|\omega + r\beta)^2$ are all positive. Consequently, a sufficient condition for $\hat{\Psi}_k > \hat{g}_k(\omega) > 0$ is that the coefficients of $\omega^{\alpha+2}$, ω^2, ω^{α} and the constant

term are all positive. Furthermore, there exists a minimal $\hat{K}_j \in N$ satisfying conditions $(H10)$–$(H12)$.Therefore, for all $k > \hat{K}_j$, we have $\hat{\Psi}_k > 0$, which implies that Eq (3.12) admits no solution. □

Let the zero solution of Eq (3.13) have $\hat{m}_{jk}$ solutions for each j and the corresponding k, and this solution is defined as $\hat{\omega}_{\hat{m}_{jk}}$.

$$\hat{\tau}^{(l)}_{\hat{m}_{jk}} = \frac{1}{\hat{\omega}_{\hat{m}_{jk}}}[\arccos A_1(\hat{\omega}_{\hat{m}_{jk}}) + 2l\pi], l = 0, 1, 2, \ldots, j = 1, 2, \ldots, n, k = 0, 1, \ldots, \hat{K}_j, \tag{3.14}$$

$$\hat{\tau}_0 = \hat{\tau}^{(0)}_{\hat{m}_{j_0k_0}} = \min_{\substack{j=1,2,\ldots,n \\ k=0,1,\ldots,\hat{K}_j}} \{\hat{\tau}^{(0)}_{\hat{m}_{jk}}\}, \hat{\omega}_0 = \hat{\omega}_{\hat{m}_{j_0k_0}}. \tag{3.15}$$

The occurrence of Hopf bifurcation must be based on the following assumptions:

$$(H13): \quad \frac{d\Phi(s)}{ds}|_{s=s_0,k=k_0,\lambda=i\hat{\omega}_0,\tau=\hat{\tau}_0} \neq 0. \tag{3.16}$$

Lemma 3.4. *Let $\lambda(\tau) = \delta(\tau) + i\omega(\tau)$ be the root of Eq (2.10) near $\tau = \hat{\tau}_0$ satisfying $\delta(\hat{\tau}_0) = 0$ and $\omega(\hat{\tau}_0) = \hat{\omega}_0$. If (3.16) holds, we have the following transversality condition:*

$$(H14): Re\left(\frac{d\lambda}{d\tau}\right)^{-1}\Big|_{k=k_0,\lambda=i\hat{\omega}_0,\tau=\hat{\tau}_0} = \frac{E_1G_1 + H_1F_1}{E_1^2 + F_1^2} \neq 0, \tag{3.17}$$

where

$$E_1 = \hat{\omega}_0^{\alpha+1}\sin\frac{\alpha\pi}{2} - a\hat{\omega}_0\sin\hat{\omega}_0\theta + \frac{r\beta\hat{\omega}_0^2}{r^2+\hat{\omega}_0^2},$$

$$F_1 = -\hat{\omega}_0^{\alpha+1}\cos\frac{\alpha\pi}{2} - a\hat{\omega}_0\cos\hat{\omega}_0\theta - dk_0^2 + \frac{r^2\beta\hat{\omega}_0}{r^2+\hat{\omega}_0^2},$$

$$G_1 = \alpha\hat{\omega}_0^{\alpha-1}\cos\frac{(\alpha-1)\pi}{2} - a\theta\cos\hat{\omega}_0\theta + \hat{\tau}_0\left(\hat{\omega}_0^{\alpha}\cos\frac{\alpha\pi}{2} + a\cos\hat{\omega}_0\theta + dk_0^2\right) + \frac{-r^2\beta\hat{\tau}_0}{r^2+\hat{\omega}_0^2} - \frac{r\beta\left(\hat{\omega}_0^2 - r^2\right)}{\left(r^2+\hat{\omega}_0^2\right)^2},$$

$$H_1 = \alpha\hat{\omega}_0^{\alpha-1}\sin\frac{(\alpha-1)\pi}{2} + a\theta\sin\hat{\omega}_0\theta + \hat{\tau}\left(\hat{\omega}_0^{\alpha}\sin\frac{\alpha\pi}{2} - a\sin\hat{\omega}_0\theta\right) + \frac{r\beta\hat{\tau}_0\omega_0}{r^2+\omega_0^2} - \frac{2r^2\beta\hat{\omega}_0}{\left(r^2+\hat{\omega}_0^2\right)^2}.$$

Proof. The derivative of Eq (2.10) with respect to τ can be obtained:

$$\frac{d\Phi(s)}{ds}\frac{ds}{d\tau} = 0.$$

Among them,

$$\frac{ds}{d\tau} = \left[\alpha\lambda^{\alpha-1}\cdot\frac{\partial\lambda}{\partial\tau} - ae^{-\lambda\theta}\theta\frac{\partial\lambda}{\partial\tau}\right]e^{\lambda\tau} + \left(\lambda^{\alpha} + ae^{-\lambda\theta} + dk^2\right)e^{\lambda\tau}\left(\frac{\partial\lambda}{\partial\tau}\cdot\tau + \lambda\right)$$
$$- \frac{r\beta e^{\lambda\tau}\left(\frac{\partial\lambda}{\partial\tau}\cdot\tau + \lambda\right)(\lambda + r) - r\beta e^{\lambda\tau}}{(\lambda+r)^2}.$$

If Eq (3.16) holds true, we can obtain

$$\left(\frac{\partial\lambda}{\partial\tau}\right)^{-1}\Bigg|_{k=k_0,\lambda=i\hat{\omega}_0,\tau=\hat{\tau}_0} = \left.\frac{\alpha\lambda^{\alpha-1} - a\theta e^{-\lambda\theta} + \left(\lambda^\alpha + ae^{-\lambda\theta} + dk^2\right)\tau - \frac{r\beta\tau}{\lambda+r} + \frac{r\beta}{(\lambda+r)^2}}{-\lambda\left(\lambda^\alpha + ae^{-\lambda\theta} + dk^2\right) + \frac{r\beta\lambda}{\lambda+r}}\right|_{k=k_0,\lambda=i\hat{\omega}_0,\tau=\hat{\tau}_0}.$$

Then it can be obtained that

$$\left(\frac{\partial\lambda}{\partial\tau}\right)^{-1}\Bigg|_{k=k_0,\lambda=i\hat{\omega}_0,\tau=\hat{\tau}_0} = \frac{E_1G_1 + H_1F_1 + i\left(E_1H_1 - G_1F_1\right)}{E_1^2 + F_1^2}.$$

Therefore, we have

$$Re(\frac{d\lambda}{d\tau})^{-1}\Big|_{k=k_0,\lambda=i\hat{\omega}_0,\tau=\hat{\tau}_0} = \frac{E_1G_1 + H_1F_1}{E_1^2 + F_1^2} \neq 0.$$

This proof is completed. □

Theorem 3.1. *Under the assumptions* $(H1)$–$(H5)$, $(H9)$, $(H13)$, *and* $(H14)$, *the following conclusions hold:*

i) If $\theta \in [0, \theta_0)$, *when* $\tau \in [0, \hat{\tau}_0)$, *the origin is asymptotically stable at system (2.4).*

ii) If $\theta \in [0, \theta_0)$, *when* $\tau = \hat{\tau}_0$, *system (2.4) undergoes a Hopf bifurcation at the origin.*

3.3. Selecting θ as the bifurcation parameter

When $\theta = 0$, Eq (2.12) can be transformed into

$$M_1e^{\lambda\tau} + M_2 = 0, \tag{3.18}$$

where

$$\begin{aligned} M_1 &= (\lambda^\alpha + a + dk^2)(\lambda + r) - r\beta, \\ M_2 &= -(\xi_j + i\eta_j)(\lambda + r). \end{aligned}$$

For simplicity, the real and imaginary parts of $M_l(\lambda)$ $(l = 1, 2)$ can be expressed as M_l^R, M_l^I, respectively. Let $\lambda = i\omega$ $(\omega > 0)$ be a pure imaginary root of Eq (3.18), and we can obtain

$$\begin{cases} M_1^R\cos\omega\tau - M_1^I\sin\omega\tau = -M_2^R, \\ M_1^R\sin\omega\tau + M_1^I\cos\omega\tau = -M_2^I, \end{cases} \tag{3.19}$$

where

$$\begin{aligned} M_1^R &= r\left(\omega^\alpha\cos\frac{\alpha\pi}{2} + a + dk^2 - \beta\right) - \omega^{\alpha+1}\sin\frac{\alpha\pi}{2}, \\ M_1^I &= \omega^{\alpha+1}\cos\frac{\alpha\pi}{2} + \left(a + dk^2\right)\omega + r\omega^\alpha\sin\frac{\alpha\pi}{2}, \\ M_2^R &= \eta_j\omega - \xi_jr, \\ M_2^I &= -\xi_j\omega - \eta_jr. \end{aligned}$$

From (3.19), we acquire

$$\begin{cases} \cos\omega\tau = \frac{-M_1^R\cdot M_2^R - M_1^I\cdot M_2^I}{(M_1^R)^2+(M_1^I)^2} = D_1(\omega), \\ \sin\omega\tau = \frac{M_1^I\cdot M_2^R - M_1^R\cdot M_2^I}{(M_1^R)^2+(M_1^I)^2} = D_2(\omega). \end{cases} \tag{3.20}$$

It can obviously be concluded from equation system (3.20) that

$$(D_1(\omega))^2 + (D_2(\omega))^2 = \frac{\left(M_2^R\right)^2 + \left(M_2^I\right)^2}{\left(M_1^R\right)^2 + \left(M_1^I\right)^2} = 1. \tag{3.21}$$

We construct a function $\bar{\Psi}_k(\omega)$ on $(0, +\infty)$ from Eq (3.21), such that the existence of its zeros directly determines the solvability of the equation. Specifically, Eq (3.21) admits a solution if and only if $\bar{\Psi}_k(\omega)$ possesses at least one positive zero.

$$\begin{aligned} \bar{\Psi}_k(\omega) =& \omega^{2\alpha+2} + 2\omega^{\alpha+2}\cos\frac{\alpha\pi}{2}\left(a+dk^2\right) + \omega^2\left(\left(a+dk^2\right)^2 - \xi_j^2 - \eta_j^2\right) + 2\omega^{\alpha+1}r\beta\sin\frac{\alpha\pi}{2} \\ &+ r^2\omega^{2\alpha} + 2r^2\left(a+dk^2-\beta\right)\omega^{\alpha}\cos\frac{\alpha\pi}{2} + r^2\left(\left(a+dk^2-\beta\right)^2 - \xi_j^2 - \eta_j^2\right). \end{aligned} \tag{3.22}$$

Lemma 3.5. *Define the root of Eq (2.11) as s_j. The following results apply characteristic equation (2.10):*

i) If there exists some $j \in \{1, 2, \ldots, n\}$ such that the following condition holds:
$(H15):\ (a-\beta)^2 < \xi_j^2 + \eta_j^2$,
then, for this specific j, the function (3.22) has at least one zero point for every $k \in \{0, 1, 2, ..., \bar{k}_T\}$. Correspondingly, Eq (3.21) has at least one positive real root, and as a consequence, the characteristic equation (2.10) admits at least one pair of pure imaginary roots.

ii) For every $j \in \{1, 2, \ldots, n\}$, there exists a sufficiently large $\bar{K}_j \in N$ that satisfies the following condition:
$(H16):\ a + dk^2 > \sqrt{\xi_j^2 + \eta_j^2 + \beta^2\sin^2\frac{\alpha\pi}{2}}$.
Under the condition, the function $\bar{\Psi}_k(\omega) > 0$ holds for all $\omega > 0$. This implies that Eq (3.21) has no positive real roots. And since k is a parameter in the characteristic equation (2.10), this further means that no solutions exist for (2.10) corresponding to $k \geqslant \bar{K}_j$.

Proof. (i) If $(a-\beta)^2 < \xi_j^2 + \eta_j^2$ for some $j \in \{1, 2, \ldots, n\}$ is established, it will exist for a particular $\bar{k}_t > 0$, making $\left(a + dk^2 - \beta\right)^2 - \xi_j^2 - \eta_j^2 = 0$.
Solving for $\bar{k}_t$, we obtain:

$$\bar{k}_t = \sqrt{\frac{\sqrt{\xi_j^2 + \eta_j^2} - a + \beta}{d}}.$$

We further define $\bar{k}_t$ to satisfy the range $\bar{k}_T < \bar{k}_t \leq \bar{k}_T + 1$ where $\bar{k}_T \in N$.
When $k = 0, 1, 2, \ldots, \bar{k}_T$, we have

$$\bar{\Psi}_k(0) = r^2\left(\left(a + dk^2 - \beta\right)^2 - \xi_j^2 - \eta_j^2\right) < 0,$$

and $\lim\limits_{\omega\to+\infty}\bar{\Psi}_k(\omega) = +\infty$. According to the zero point theorem, Eq (3.21) must have a positive root, that is, Eq (2.10) has a pair of pure imaginary roots.

(ii) To prove (ii), we transform Eq (3.22) into the following equivalent form:

$$\begin{aligned}\bar{\Psi}_k(\omega) =&\omega^{2\alpha+2} + 2\omega^{\alpha+2}\cos\frac{\alpha\pi}{2}\left(a + dk^2\right) + \omega^2\left(\left(a + dk^2\right)^2 - \xi_j^2 - \eta_j^2 - \beta^2\sin^2\frac{\alpha\pi}{2}\right)\\ &+ \left(\omega\beta\sin\frac{\alpha\pi}{2} + r\omega^\alpha\right)^2 + 2r^2\left(a + dk^2 - \beta\right)\omega^\alpha\cos\frac{\alpha\pi}{2}\\ &+ r^2\left(\left(a + dk^2 - \beta\right)^2 - \xi_j^2 - \eta_j^2\right).\end{aligned} \tag{3.23}$$

For $\omega > 0$, the terms $\omega^{2\alpha+2}$ and $\left(\omega\beta\sin\frac{\alpha\pi}{2} + r\omega^\alpha\right)^2$ are inherently positive. Therefore, a sufficient condition for $\bar{\Psi}_k(\omega) > 0$ is that the coefficients of the $\omega^{\alpha+2}$, ω^2 and ω^α terms, along with the constant term, are all positive. Furthermore, there exists a minimal $\bar{K}_j \in N$ satisfying condition $(H16)$. Consequently, for all $k \geqslant \bar{K}_j$, we have $\bar{\Psi}_k(\omega) > 0$, which implies that Eq (3.21) admits no solution.

□

Let the zero solution of Eq (3.22) have $\bar{m}_{jk}$ solutions for each j and the corresponding k, and this solution is defined as $\omega_{\bar{m}_{jk}}$.

$$\bar{\tau}^{(l)}_{\bar{m}_{jk}} = \frac{1}{\bar{\omega}_{\bar{m}_{jk}}}[\arccos D_1(\bar{\omega}_{\bar{m}_{jk}}) + 2l\pi], l = 0, 1, 2, \ldots, j = 1, 2, \ldots, n, k = 0, 1, \ldots, \bar{K}_j, \tag{3.24}$$

$$\bar{\tau}_0 = \bar{\tau}^{(0)}_{\bar{m}_{j_0k_0}} = \min_{\substack{j=1,2,\ldots,n\\ k=0,1,\ldots,\bar{K}_j}}\{\tau^{(0)}_{\bar{m}_{jk}}\}, \bar{\omega}_0 = \bar{\omega}_{\bar{m}_{j_0k_0}}. \tag{3.25}$$

When $\tau \in [0, \tau_0)$, $\theta > 0$, Eq (12) can be transformed into

$$N_1e^{-\lambda\theta} + N_2 = 0, \tag{3.26}$$

where

$$\begin{aligned}N_1 &= ae^{\lambda\tau}(\lambda + r),\\ N_2 &= ((\lambda^\alpha + dk^2)(\lambda + r) - r\beta)e^{\lambda\tau} - (\xi_j + i\eta_j)(\lambda + r).\end{aligned}$$

For simplicity, the real and imaginary parts of $N_l(\lambda)$ $(l = 1, 2)$ can be expressed as N_l^R, N_l^I, respectively. Substituting $\lambda = i\omega$ $(\omega > 0)$ into (3.26) holds for some $j \in \{1, 2, \cdots, n\}$

$$\begin{cases}N_1^R\cos\omega\theta + N_1^I\sin\omega\theta = -N_2^R,\\ N_1^I\cos\omega\theta - N_1^R\sin\omega\theta = -N_2^I,\end{cases} \tag{3.27}$$

where

$$\begin{aligned}N_1^R &= ar\cos\omega\tau - a\omega\sin\omega\tau,\\ N_1^I &= ar\sin\omega\tau + a\omega\cos\omega\tau,\\ N_2^R &= \left(r\left(\omega^\alpha\cos\frac{\alpha\pi}{2} + dk^2\right) - \omega^{\alpha+1}\sin\frac{\alpha\pi}{2} - r\beta\right)\cos\omega\tau - \left(\omega\left(\omega^\alpha\cos\frac{\alpha\pi}{2} + dk^2\right) + r\omega^\alpha\sin\frac{\alpha\pi}{2}\right)\\ &\quad\times\sin\omega\tau - \left(\xi_jr - \eta_j\omega\right),\\ N_2^I &= \left(r\left(\omega^\alpha\cos\frac{\alpha\pi}{2} + dk^2\right) - \omega^{\alpha+1}\sin\frac{\alpha\pi}{2} - r\beta\right)\sin\omega\tau + \left(\omega\left(\omega^\alpha\cos\frac{\alpha\pi}{2} + dk^2\right) + r\omega^\alpha\sin\frac{\alpha\pi}{2}\right)\\ &\quad\times\cos\omega\tau - \left(\xi_j\omega + \eta_jr\right).\end{aligned}$$

From (3.27), we acquire

$$\begin{cases} \cos\omega\theta = \frac{-N_1^R\cdot N_2^R - N_1^I\cdot N_2^I}{(N_1^R)^2+(N_1^I)^2} = C_1(w), \\ \sin\omega\theta = \frac{-N_1^I\cdot N_2^R + N_1^R\cdot N_2^I}{(N_1^R)^2+(N_1^I)^2} = C_2(w). \end{cases} \tag{3.28}$$

It can obviously be concluded from equation system (3.28) that

$$(C_1(\omega))^2 + (C_2(\omega))^2 = \frac{\left(N_2^R\right)^2 + \left(N_2^I\right)^2}{\left(N_1^R\right)^2 + \left(N_1^I\right)^2} = 1. \tag{3.29}$$

We construct a function $\tilde{\Psi}_k(\omega)$ on $(0, +\infty)$ from Eq (3.29), such that the existence of its zeros directly determines the solvability of the equation. Specifically, Eq (3.29) admits a solution if and only if $\tilde{\Psi}_k(\omega)$ possesses at least one positive zero.

$$\begin{aligned} \tilde{\Psi}_k(\omega) =& P^2 + Q^2 + \left(\xi_j^2 + \eta_j^2 - a^2\right)\left(\omega^2 + r^2\right) - 2\left(P\xi_j + Q\eta_j\right)(r\cos\omega\tau + \omega\sin\omega\tau) \\ &+ 2\left(P\eta_j - Q\xi_j\right)(\omega\cos\omega\tau - r\sin\omega\tau), \end{aligned} \tag{3.30}$$

where

$$\begin{aligned} P &= r\omega^\alpha\cos\frac{\alpha\pi}{2} + rdk^2 - \omega^{\alpha+1}\sin\frac{\alpha\pi}{2} - r\beta, \\ Q &= \omega^{\alpha+1}\cos\frac{\alpha\pi}{2} + \omega dk^2 + r\omega^\alpha\sin\frac{\alpha\pi}{2}. \end{aligned}$$

Lemma 3.6. *Define the root of Eq (2.11) as s_j. The following results apply characteristic equation (2.10):*

i) If there exists some $j \in \{1, 2, \ldots, n\}$ such that the following condition holds:
$(H17)$: $(\xi_j + \beta)^2 < a^2 - \eta_j^2$,
then, for this specific j, the function (3.30) has at least one zero point for every $k \in \{0, 1, 2, ..., \tilde{k}_T\}$. Correspondingly, Eq (3.29) has at least one positive real root, and as a consequence, the characteristic equation (2.10) admits at least one pair of pure imaginary roots.

ii) For every $j \in \{1, 2, \ldots, n\}$, there exists a sufficiently large $\tilde{K}_j \in N$ that satisfies the following condition:
$(H18)$: $dk^2 - \sqrt{\left(\sqrt{\xi_1^2 + \eta_j^2} + |a|\right)^2 + \beta^2\sin^2\frac{\alpha\pi}{2}} > 0$.
Under the condition, the function $\tilde{\Psi}_k(\omega) > 0$ holds for all $\omega > 0$. This implies that Eq (3.29) has no positive real roots. And since k is a parameter in the characteristic equation (2.10), this further means that no solutions exist for (2.10) corresponding to $k \geqslant \tilde{K}_j$.

Proof. (i) If $(\xi_j + \beta)^2 < a^2 - \eta_j^2$ for some $j \in \{1, 2, \ldots, n\}$ is established, it will exist for a particular $\tilde{k}_t > 0$, making $(dk_t^2 - \xi_j - \beta)^2 + \eta_j^2 - a^2 = 0$.
Solving for $\tilde{k}_t$, we obtain:

$$\tilde{k}_t = \sqrt{\frac{\sqrt{a^2 - \eta_j^2} + \xi_j + \beta}{d}}.$$

We further define $\tilde{k}_t$ to satisfy the range $\tilde{k}_T < \tilde{k}_t \leq \tilde{k}_T + 1$ where $\tilde{k}_T \in N$.
When $k = 0, 1, 2, \ldots, k_T$, we have

$$\tilde{\Psi}_k(0) = r^2\left((dk^2 - \xi_j - \beta)^2 + \eta_j^2 - a^2\right) < 0,$$

and $\lim\limits_{\omega\to+\infty} \tilde{\Psi}_k(\omega) = +\infty$. According to the zero point theorem, Eq (3.29) must have a positive root, that is, Eq (2.10) has a pair of pure imaginary roots.

(ii) We now analyze the combined trigonometric terms of $\tilde{\Psi}_k(\omega)$:

$$\begin{aligned}&-2\left(P\xi_j + Q\eta_j\right)(r\cos\omega\tau + \omega\sin\omega\tau) + 2\left(P\eta_j - Q\xi_j\right)(\omega\cos\omega\tau - r\sin\omega\tau)\\ =&-2\left(P\xi_j + Q\eta_j\right)O + 2\left(P\eta_j - Q\xi_j\right)Z,\end{aligned}$$

where

$$\begin{aligned}O =& r\cos\omega\tau + \omega\sin\omega\tau,\\ Z =& \omega\cos\omega\tau - r\sin\omega\tau.\end{aligned}$$

It can be obtained from the Cauchy–Schwarz inequality that

$$\left|-\left(P\xi_j + Q\eta_j\right)O + \left(P\eta_j - Q\xi_j\right)Z\right| \leq \sqrt{\left(P\xi_j + Q\eta_j\right)^2 + \left(P\eta_j - Q\xi_j\right)^2}\sqrt{O^2 + Z^2}. \tag{3.31}$$

Among them,

$$\begin{aligned}O^2 + Z^2 &= \omega^2 + r^2,\\ \left(P\xi_j + Q\eta_j\right)^2 + \left(P\eta_j - Q\xi_j\right)^2 &= \left(P^2 + Q^2\right)\left(\xi_j^2 + \eta_j^2\right).\end{aligned}$$

According to Eq (3.31), it can be obtained that

$$\tilde{\Psi}_k(\omega) \geqslant \left(P^2 + Q^2\right) + \left(\xi_j^2 + \eta_j^2 - a^2\right)\left(\omega^2 + r^2\right) - 2\sqrt{\left(P^2 + Q^2\right)\left(\xi_j^2 + \eta_j^2\right)}\cdot\sqrt{\omega^2 + r^2}.$$

Construct a function $\tilde{g}_k(\omega)$

$$\begin{aligned}\tilde{g}_k(\omega) &= \left(P^2 + Q^2\right) + \left(\xi_j^2 + \eta_j^2 - a^2\right)\left(\omega^2 + r^2\right) - 2\sqrt{\left(P^2 + Q^2\right)\left(\xi_j^2 + \eta_j^2\right)}\sqrt{\omega^2 + r^2}\\ &= \left(\sqrt{P^2 + Q^2} - \sqrt{\left(\xi_j^2 + \eta_j^2\right)}\sqrt{\omega^2 + r^2}\right)^2 - a^2\left(\omega^2 + r^2\right)\\ &= \left(\sqrt{P^2 + Q^2} - \left(\sqrt{\xi_j^2 + \eta_j^2} - |a|\right)\sqrt{\omega^2 + r^2}\right)\left(\sqrt{P^2 + Q^2}\right.\\ &\left.- \left(\sqrt{\xi_j^2 + \eta_j^2} + |a|\right)\sqrt{\omega^2 + r^2}\right).\end{aligned} \tag{3.32}$$

We now analyze the conditions under which $\tilde{g}_k(\omega) > 0$. Consider the inequality

$$P^2 + Q^2 > \left(\xi_i^2 + \eta_j^2 + a^2 + 2\sqrt{\xi_j^2 + \eta_j^2}\cdot|a|\right)\left(\omega^2 + r^2\right). \tag{3.33}$$

Expand on the above inequality

$$\omega^{2\alpha+2} + 2\omega^{\alpha+2}dk^2\cos\frac{\alpha\pi}{2} + 2\omega^{\alpha+1}r\beta\sin\frac{\alpha\pi}{2} + \omega^{2\alpha}\cdot r^2 + \left(\left(dk^2\right)^2 - \left(\sqrt{\xi_j^2+\eta_j^2}+|a|\right)^2\right)$$
$$\times\,\omega^2 + 2\omega^{\alpha}\cos\frac{\alpha\pi}{2}\cdot r^2\left(dk^2-\beta\right) + r^2\left(\left(dk^2-\beta\right)^2 - \left(\sqrt{\xi_j^2+\eta_j^2}+|a|\right)^2\right) > 0.$$

Complete the square for some terms on the left side of the inequality

$$\omega^{2\alpha+2} + 2\omega^{\alpha+2}dk^2\cos\frac{\alpha\pi}{2} + \left(\left(dk^2\right)^2 - \left(\sqrt{\xi_i^2+\eta_j^2}+|a|\right)^2 - \beta^2\sin^2\frac{\alpha\pi}{2}\right)\omega^2$$
$$+\left(\omega^{\alpha}r + \omega\beta\sin\frac{\alpha\pi}{2}\right)^2 + 2\omega^{\alpha}\cos\frac{\alpha\pi}{2}\cdot r^2\left(dk^2-\beta\right) + r^2\left(\left(dk^2-\beta\right)^2 - \left(\sqrt{\xi_j^2+\eta_j^2}+|a|\right)^2\right) > 0.$$

When $\left(dk^2\right)^2-\left(\sqrt{\xi_i^2+\eta_j^2}+|a|\right)^2-\beta^2\sin^2\frac{\alpha\pi}{2}\geqslant 0$, inequality (3.33) is satisfied. Under this condition, we have:

$$\sqrt{P^2+Q^2} > \left(\sqrt{\xi_j^2+\eta_j^2}+|a|\right)\sqrt{\omega^2+r^2},$$

which implies

$$\sqrt{P^2+Q^2} - \left(\sqrt{\xi_j^2+\eta_j^2}-|a|\right)\sqrt{\omega^2+r^2} > 0,$$

and consequently $\tilde{g}_k(\omega) > 0$. Furthermore, there exists a minimum $\tilde{K}_j \in N$ satisfying condition $(H18)$ such that when $k \geqslant \tilde{K}_j$, the function $\tilde{\Psi}_k(\omega) > 0$, and Eq (3.29) has no solution.

□

Let the zero solution of Eq (3.30) have $\tilde{m}_{jk}$ solutions for each j and the corresponding k, and this solution is defined as $\omega_{\tilde{m}_{jk}}$.

$$\tilde{\theta}^{(l)}_{\tilde{m}_{jk}} = \frac{1}{\tilde{\omega}_{\tilde{m}_{jk}}}[\arccos C_1(\tilde{\omega}_{\tilde{m}_{jk}}) + 2l\pi], l = 0, 1, 2, \ldots, j = 1, 2, \ldots, n, k = 0, 1, \ldots, \tilde{K}_j, \tag{3.34}$$

$$\tilde{\theta}_0 = \tilde{\theta}^{(0)}_{\tilde{m}_{j_0k_0}} = \min_{\substack{j=1,2,\ldots,n\\ k=0,1,\ldots,\tilde{K}_j}}\{\tilde{\theta}^{(0)}_{\tilde{m}_{jk}}\}, \omega_0 = \omega_{\tilde{m}_{j_0k_0}}. \tag{3.35}$$

Lemma 3.7. *Let $\lambda(\theta) = \delta(\theta) + i\omega(\theta)$ be the root of Eq (2.10) near $\theta = \tilde{\theta}_0$ satisfying $\delta(\tilde{\theta}_0) = 0$ and $\omega(\tilde{\theta}_0) = \tilde{\omega}_0$. If (3.16) holds, we have the following transversality condition:*

$$(H20):\ Re\left(\frac{d\lambda}{d\theta}\right)^{-1}\Bigg|_{k=k_0,\lambda=i\tilde{\omega}_0,\theta=\tilde{\theta}_0} = \frac{\tilde{E}_1\tilde{G}_1 + \tilde{H}_1\tilde{F}_1}{\tilde{E}_1^2+\tilde{F}_1^2} \neq 0, \tag{3.36}$$

where

$$\tilde{E}_1 = a\tilde{\omega}_0 \sin\tilde{\omega}_0\tilde{\theta}_0 - \frac{r\beta\left(\tilde{\omega}_0^2 + r^2\right)}{\left(\tilde{\omega}_0^2 + r^2\right)^2 + 4\tilde{\omega}_0^2 r^2},$$

$$\tilde{F}_1 = a\tilde{\omega}_0 \cos\tilde{\omega}_0\tilde{\theta}_0 + \frac{2\tilde{\omega}_0 r}{\left(\tilde{\omega}_0^2 + r^2\right) + 4\tilde{\omega}_0^2 r^2},$$

$$\tilde{G}_1 = a\left(\tau - \tilde{\omega}_0\right)\cos\tilde{\omega}_0\tilde{\theta}_0 + \alpha\tilde{\omega}_0^{\alpha-1}\cos\frac{(\alpha-1)\pi}{2} + \tau\left(\tilde{\omega}_0^{\alpha}\cos\frac{\alpha\pi}{2} + dk^2 - \frac{r^2\beta}{\tilde{\omega}_0^2 + r^2}\right),$$

$$\tilde{H}_1 = -a\left(\tau - \theta_0\right)\sin\tilde{\omega}_0\tilde{\theta}_0 + \alpha\tilde{\omega}_0^{\alpha-1}\sin\frac{(\alpha-1)\pi}{2} + \tau\left(\omega_0^{\alpha}\sin\frac{\alpha\pi}{2} + \frac{r\beta\tilde{\omega}_0}{\tilde{\omega}_0^2 + r^2}\right).$$

Proof. The derivative of Eq (2.10) with respect to θ can be obtained:

$$\frac{d\Phi(s)}{ds}\frac{ds}{d\theta} = 0.$$

If Eq (3.16) holds true, we can obtain

$$\frac{ds}{d\theta} = \left(ae^{\lambda\tau}\cdot\tau\cdot\frac{\partial\lambda}{\partial\theta}\right)e^{-\lambda\theta} - ae^{\lambda\tau}\cdot e^{-\lambda\theta}\left(\theta\cdot\frac{\partial\lambda}{\partial\theta} + \lambda\right) + \left(\alpha\lambda^{\alpha-1}\frac{\partial\lambda}{\partial\theta} + \frac{r\beta}{(\lambda+r)^2}\right)e^{\lambda\tau}$$
$$+ \left(\lambda^{\alpha} + \alpha k^2 - \frac{r\beta}{\lambda+r}\right)e^{\lambda\tau}\cdot\tau\cdot\frac{d\lambda}{d\theta} = 0.$$

According to Lemma 3.4's proof, the same principle applies

$$Re\left(\frac{d\lambda}{d\theta}\right)^{-1}\Bigg|_{k=k_0,\lambda=i\tilde{\omega}_0,\theta=\tilde{\theta}_0} = \frac{\tilde{E}_1\tilde{G}_1 + \tilde{H}_1\tilde{F}_1}{\tilde{E}_1^2 + \tilde{F}_1^2} \neq 0.$$

This proof is completed. □

Theorem 3.2. *Under the assumptions* $(H1)$–$(H4)$, $(H13)$, $(H15)$, $(H17)$, *and* $(H20)$, *the following conclusions hold:*

i) If $\tau \in [0, \bar{\tau}_0)$, *when* $\theta \in [0, \tilde{\theta}_0)$, *the origin is asymptotically stable at system (2.4).*

ii) If $\tau \in [0, \bar{\tau}_0)$, *when* $\theta = \tilde{\theta}_0$, *system (2.4) undergoes a Hopf bifurcation at the origin.*

Remark 3.3. *When* $d = 0$, *system (2.4) will degenerate into the ring neural network studied in [40]. This paper further expands on this basis. It extends the dynamic behavior of neuronal activities that only varies with time to a reaction-diffusion system that simultaneously depends on temporal evolution and spatial diffusion. This expansion makes the model more physiologically practical and is an important supplement and improvement to the existing theory.*

4. Numerical simulations

In this section, Examples 1 and 2 are respectively used to verify the correctness of Theorems 3.1 and 3.2. We will use $tanh(\cdot)$ as the activation function for $f_{ij}(\cdot)$ and $g_i(\cdot)$. We consider a ring neural network with three neurons. The initial conditions are $y_1(x,t) = 0.025\cos(4x)$, $y_2(x,t) = 0.03\cos(3x)$, and $y_3(x,t) = 0.05\cos(2x)$. This situation can be regarded as several tiny random disturbances around the equilibrium state $E^* = (0, 0, \ldots, 0)^T$.

4.1. Example 1

In this example, we study the bifurcation problem caused by τ by fixing θ. The parameters we selected are as follows: $\alpha = 0.95$, $d = 1$, $r = 0.1$, $\beta = -0.1$, $a = 1.8$, $b_{12} = -1.7$, $b_{21} = -0.4$, $b_{13} = -2$, $b_{31} = -1.1$, $b_{23} = -2$, and $b_{32} = -1.2$.

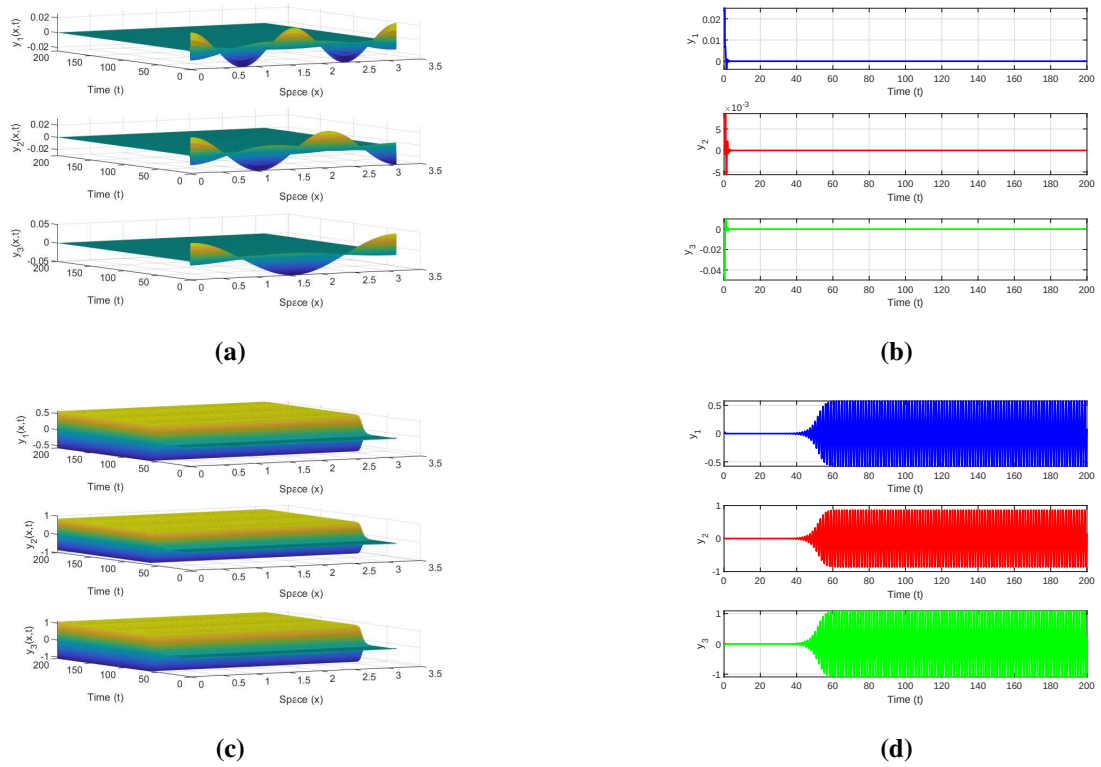

(a) **(b)** **(c)** **(d)**

Figure 3. (a),(b) When $\tau = 0.23 < \hat{\tau}_0$, the trivial equilibrium points of the network are locally asymptotically stable. (c),(d) When $\tau = 0.31 > \hat{\tau}_0$, the trivial equilibrium point of the network is unstable.

The three roots of Eq (2.11) are obtained through direct computation, yielding $Max\xi_j \approx 1.3276$ for $j = 1, 2, 3$. Given that $a = 1.8 > 1.3276$ and $\beta < 0$, the assumptions of Lemma 3.1 are satisfied. We further compute $\omega_0 \approx 1.4519$ and the critical delay $\theta_0 \approx 0.5714$. Setting $\theta = 0.45 \in [0, \theta_0]$, we solve for $\hat{\omega}_0 \approx 4.5537$ and the corresponding bifurcation point $\hat{\tau}_0 \approx 0.3036$. In accordance with Theorem 3.2, the trivial equilibrium of the network is locally asymptotically stable when $\tau = 0.23 < \hat{\tau}_0$, as illustrated in Figure 3(a),(b). Conversely, when $\tau = 0.31 > \hat{\tau}_0$, the equilibrium becomes unstable, as shown in Figure 3(c),(d).

As shown in Figure 4(a), under the condition that $\tau = 0$, the critical value of the network Hopf bifurcation θ_0 exhibits a gradually decreasing trend as the self-feedback coefficient a increases continuously. As shown in Figure 4(b), a horizontal comparison reveals that when the leakage delay θ increases from 0 to 0.5, the first Hopf bifurcation point of the network exhibits a monotonically decreasing trend. This indicates that an increase in the leakage delay θ can promote the earlier occurrence of Hopf bifurcation. In addition, a vertical comparison shows that when $\theta < 0.2$, increasing the self-feedback coefficient tends to delay the onset of bifurcation. Notably, when the leakage delay

$\theta > 0.25$, the trend of the curve changes significantly; thereafter, as the parameter a increases, the Hopf bifurcation point $\hat{\tau}_0$ decreases gradually.

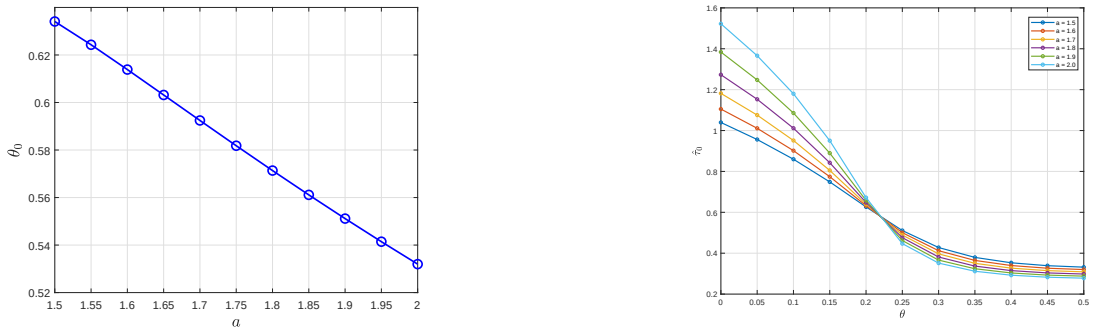

(a) **(b)**

Figure 4. (a) Effect of the self-feedback coefficient a on the network Hopf bifurcation point θ_0 when $\tau = 0$. (b) Effects of the leakage delay θ and self-feedback coefficient a on the network Hopf bifurcation point $\hat{\tau}_0$.

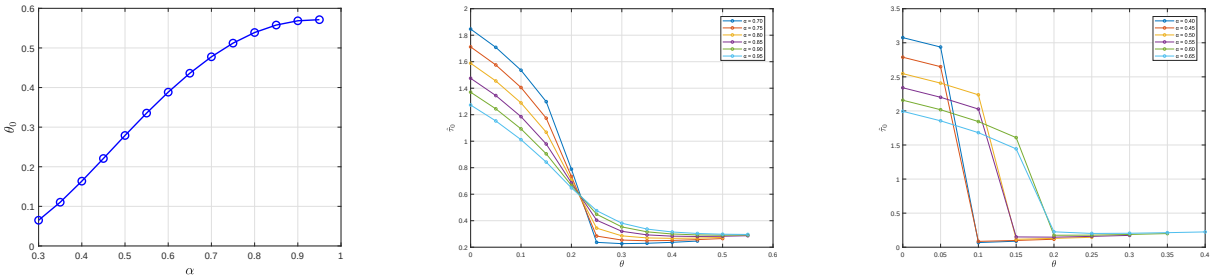

(a) **(b)** **(c)**

Figure 5. (a) Influence of fractional-order α on the Hopf bifurcation point θ_0 (with $\tau = 0$). (b) Combined effects of leakage delay θ and fractional-order α (ranging from 0.7 to 0.95) on the Hopf bifurcation point $\hat{\tau}_0$. (c) Combined effects of leakage delay θ and fractional-order α (ranging from 0.4 to 0.65) on the Hopf bifurcation point $\hat{\tau}_0$.

Figure 5(a) illustrates the impact of the fractional-order α (ranging from 0.3 to 0.95) on the Hopf bifurcation point θ_0 under the condition of $\tau = 0$. θ_0 exhibits a continuous upward trend as α increases. This pattern indicates that a larger α leads to a higher threshold of θ_0 required for the system to undergo Hopf bifurcation. Figure 5(b) focuses on the interval $\alpha \in [0.7, 0.95]$, where the relationship between the leakage delay θ and the bifurcation point $\hat{\tau}_0$ shows a trend of first decreasing and then stabilizing. Figure 5(c) corresponds to the low fractional-order interval $\alpha \in [0.4, 0.65]$. Its variation trend is similar to that in the interval $\alpha \in [0.7, 0.95]$, while the decreasing process is notably steeper.

4.2. Example 2

In this example, we study the bifurcation problem caused by θ by fixing τ. We utilize the parameter set from Example 1.

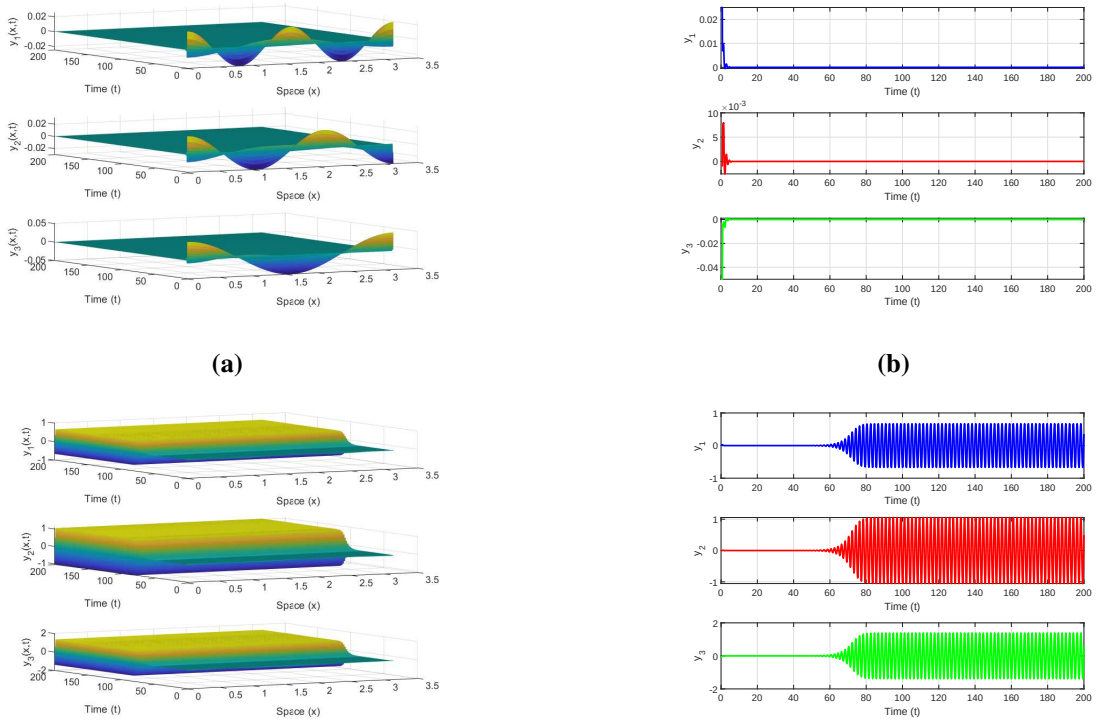

Figure 6. (a),(b) When $\theta = 0.11 < \tilde{\theta}_0$, the trivial equilibrium points of the network are locally asymptotically stable. (c),(d) When $\theta = 0.2 > \tilde{\theta}_0$, the trivial equilibrium point of the network is unstable.

As established in Example 1, the chosen parameters satisfy the conditions of Lemma 3.1. We further compute $\bar{\omega}_0 \approx 1.8788$ and the critical delay $\bar{\tau}_0 \approx 1.2731$. Setting $\tau = 0.7 \in [0, \bar{\tau}_0]$, we solve for $\tilde{\omega}_0 \approx 3.2497$ and the corresponding bifurcation point $\tilde{\theta}_0 \approx 0.1869$. In accordance with Theorem 3.2, the trivial equilibrium of the network is locally asymptotically stable when $\theta = 0.11 < \tilde{\theta}_0$, as illustrated in Figure 6(a),(b). Conversely, when $\theta = 0.2 > \tilde{\theta}_0$, the equilibrium becomes unstable, as shown in Figure 6(c),(d).

As shown in Figure 7(a), under the condition that $\theta = 0$, the critical value of the network Hopf bifurcation $\hat{\tau}_0$ exhibits a gradually increasing trend as the self-feedback coefficient a increases continuously. As shown in Figure 7(b), the system exhibits distinct stage-specific dynamic characteristics. Specifically, the leakage time delay $\tilde{\theta}_0$ increases continuously as τ rises; when τ increases to a certain value, $\tilde{\theta}_0$ decreases gradually with the increase of τ. The essence of this phenomenon lies in the following: Within the interval where τ is increasing, the pure real root solution fails to generate a positive $\tilde{\omega}_0$ solution for any wavenumber k, and at this stage, the $\tilde{\omega}_0$ solution is entirely determined by the complex conjugate roots. However, when τ reaches a critical value, the pure real root solution begins to produce positive $\tilde{\omega}_0$ solutions and gets activated. Since the minimum $\tilde{\theta}_0$ corresponding to the pure real root solution is significantly smaller than that of the complex conjugate root solution, the system experiences a sharp drop in $\tilde{\theta}_0$ at this critical value of τ. A vertical comparison reveals that when the leakage delay $\theta < 0.6$, increasing the self-feedback coefficient a can accelerate the occurrence of Hopf bifurcation; whereas

when $\theta > 0.6$, an increase in the self-feedback coefficient a will lead to a gradual increase in the Hopf bifurcation point $\hat{\tau}_0$.

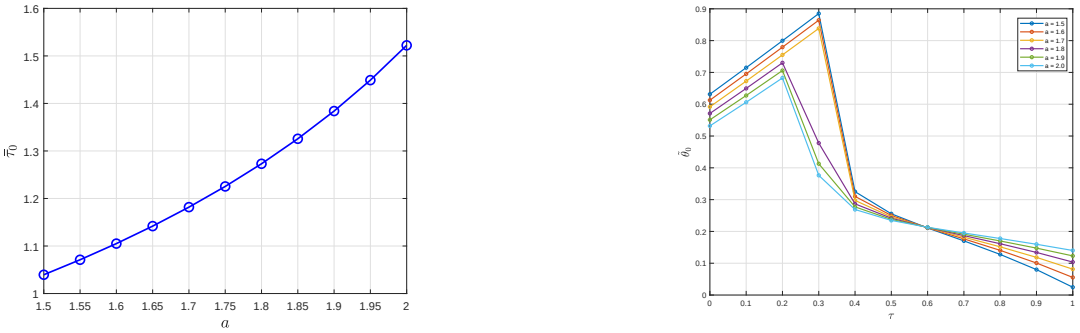

(a) **(b)**

Figure 7. (a) Effect of the self-feedback coefficient a on the network Hopf bifurcation point $\bar{\tau}_0$ when $\theta = 0$. (b) Effects of the delay τ and self-feedback coefficient a on the network Hopf bifurcation point $\tilde{\theta}_0$.

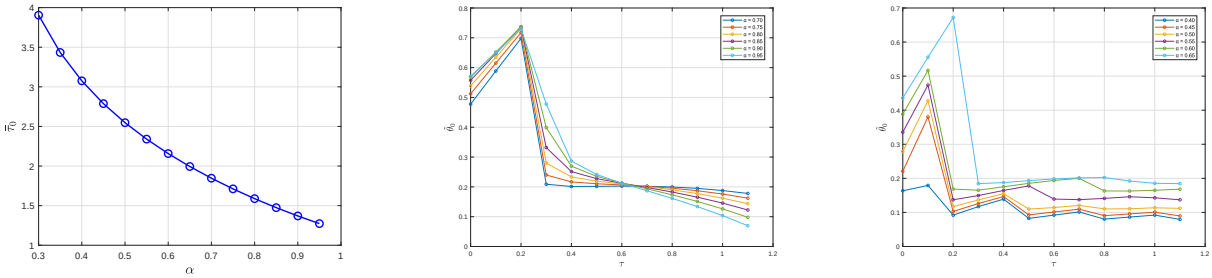

(a) **(b)** **(c)**

Figure 8. (a) Influence of fractional-order α on the Hopf bifurcation point $\bar{\tau}_0$ (with $\theta = 0$). (b) Combined effects of leakage delay τ and fractional-order α (ranging from 0.7 to 0.95) on the Hopf bifurcation point $\tilde{\theta}_0$. (c) Combined effects of leakage delay τ and fractional-order α (ranging from 0.4 to 0.65) on the Hopf bifurcation point $\tilde{\theta}_0$.

Figure 8 characterizes the influence of the fractional-order α and leakage delay τ on the Hopf bifurcation point $\tilde{\theta}_0$. Figure 8(a) illustrates the effect of the fractional-order α (ranging from 0.3 to 1) on the Hopf bifurcation point $\bar{\tau}_0$ under the condition $\theta = 0$. $\bar{\tau}_0$ shows a downward trend as α increases, which means a larger α corresponds to a lower $\bar{\tau}_0$ threshold required for the system to undergo Hopf bifurcation. Figure 8(b) focuses on the interval $\alpha \in [0.7, 0.95]$, where the relationship between the leakage delay τ and the bifurcation point $\tilde{\theta}_0$ follows a rising-then-falling pattern. For Figure 8(c), which corresponds to the low fractional-order interval $\alpha \in [0.4, 0.65]$, $\tilde{\theta}_0$ exhibits a fluctuating trend of repeated rises and falls as τ changes. Compared with Figure 8(c), $\tilde{\theta}_0$ shows greater volatility in its response to τ in the low fractional-order region.

5. Conclusions

This paper studied a class of multi-delay bidirectional ring neural networks based on reaction–diffusion equations. For the bifurcation problem caused by two unequal delays, a general analysis method was proposed. The characteristic equation of the system was derived by applying the Coates formula, the stability of the network at the trivial equilibrium point was analyzed, and the bifurcation behavior caused by two time delays was systematically studied. Theoretical results showed that when the time lag exceeds a certain critical value, the system will generate a series of periodic oscillation phenomena near the steady state. The numerical experiments further verified the correctness and validity of the theoretical analysis. In subsequent research, we will introduce a bifurcation control strategy to optimize the dynamic performance of the reaction-diffusion neural network.

Use of AI tools declaration

The author declares that she has not used Artificial Intelligence (AI) tools in the creation of this article.

Acknowledgments

The author sincerely thanks all the teachers in the editorial department and the anonymous reviewers for their precious time and constructive suggestions, which have significantly improved the quality of this article.

Conflict of interest

The author declare there is no conflicts of interest.

References

1. L. Pantanowitz, T. Pearce, I. Abukhiran, M. Hanna, S. Wheeler, T. R. Soong, et al., Nongenerative artificial intelligence in medicine: advancements and applications in supervised and unsupervised machine learning, *Mod. Pathol.*, **38** (2025), 100680. https://doi.org/10.1016/j.modpat.2024.100680
2. Y. H. Hu, X. L. Xu, L. Duan, M. Bilal, Q. Y. Wang, W. C. Dou, End-edge collaborative inference of convolutional fuzzy neural networks for big data-driven internet of things, *IEEE Trans. Fuzzy Syst.*, **33** (2025), 203–217. https://doi.org/10.1109/tfuzz.2024.3412971
3. Y. X. He, E. Zio, Z. M. Yang, Q. Xiang, L. Fan, Q. He, et al., A systematic resilience assessment framework for multi-state systems based on physics-informed neural network, *Reliab. Eng. Syst. Saf.*, **257** (2025), 110866. https://doi.org/10.1016/j.ress.2025.110866
4. J. H. Ma, H. L. Tu, Analysis of the stability and Hopf bifurcation of money supply delay in complex macroeconomic models, *Nonlinear Dyn.*, **76** (2013), 497–508. https://doi.org/10.1007/s11071-013-1143-x
5. C. J. Xu, W. Ou, Q. Y. Cui, Y. C. Pang, M. X. Liao, J. W. Shen, et al., Theoretical exploration and controller design of bifurcation in a plankton population dynamical system accompanying delay, *Discrete Contin. Dyn. Syst. - Ser. S*, **18** (2025), 1182–1211. https://doi.org/10.3934/dcdss.2024036

6. C. J. Xu, W. Ou, Y. C. Pang, Q. Y. Cui, M. Rahman, M. Farman, et al., Hopf bifurcation control of a fractional-order delayed turbidostat model via a novel extended hybrid controller, *Match-Commun. Math. Comput. Chem.*, **91** (2023), 367–413. https://doi.org/10.30546/1683-6154.22.4.2023.495
7. P. Baldi, A. F. Atiya, How delays affect neural dynamics and learning, *IEEE Trans. Neural Networks*, **5** (1994), 612–621. https://doi.org/10.1109/72.298231
8. T. Y. Cai, H. G. Zhang, F. S. Yang, Simplified frequency method for stability and bifurcation of delayed neural networks in ring structure, *Neurocomputing*, **121** (2013), 416–422. https://doi.org/10.1016/j.neucom.2013.05.022
9. C. D. Huang, J. D. Cao, M. Xiao, A. Alsaedi, T. Hayat, Effects of time delays on stability and Hopf bifurcation in a fractional ring-structured network with arbitrary neurons, *Commun. Nonlinear Sci. Numer. Simul.*, **57** (2018), 1–13. https://doi.org/10.1016/j.cnsns.2017.09.005
10. X. Xu, D. Y. Yu, Z. H. Wang, Inter-layer synchronization of periodic solutions in two coupled rings with time delay, *Physica D*, **396** (2019), 1–11. https://doi.org/10.1016/j.physd.2019.02.010
11. B. B. Tao, M. Xiao, W. X. Zheng, J. D. Cao, J. W. Tang, Dynamics analysis and design for a bidirectional super-ring-shaped neural network with n neurons and multiple delays, *IEEE Trans. Neural Networks Learn. Syst.*, **32** (2021), 2978–2992. https://doi.org/10.1109/tnnls.2020.3009166
12. R. T. Xing, M. Xiao, Y. Z. Zhang, J. L. Qiu, Stability and Hopf bifurcation analysis of an (n + m)-neuron double-ring neural network model with multiple time delays, *J. Syst. Sci. Complexity*, **35** (2021), 159–178. https://doi.org/10.1007/s11424-021-0108-2
13. C. A. Desoer, The optimum formula for the gain of a flow graph or a simple derivation of Coates' formula, *Proc. IRE*, **48** (1960), 883–889. https://doi.org/10.1109/jrproc.1960.287625
14. Q. Dai, Exploration of bifurcation and stability in a class of fractional-order super-double-ring neural network with two shared neurons and multiple delays, *Chaos, Solitons Fractals*, **168** (2023), 113185. https://doi.org/10.1016/j.chaos.2023.113185
15. Y. Z. Zhang, M. Xiao, W. X. Zheng, J. D. Cao, Large-scale neural networks with asymmetrical three-ring structure: stability, nonlinear oscillations, and Hopf bifurcation, *IEEE Trans. Cybern.*, **52** (2022), 9893–9904. https://doi.org/10.1109/tcyb.2021.3109566
16. H. S. Hou, C. Luo, Z. W. Mo, On fractional ring neural networks with multiple time delays: stability and Hopf bifurcation analysis, *Chin. J. Phys.*, **90** (2024), 303–318. https://doi.org/10.1016/j.cjph.2024.05.030
17. Y. Z. Zhang, M. Xiao, J. D. Cao, W. X. Zheng, Stability and Hopf bifurcation for a quaternion-valued three-neuron neural network with leakage delay and communication delay, *J. Franklin Inst.*, **360** (2023), 12969–12989. https://doi.org/10.1016/j.jfranklin.2023.09.052
18. H. L. Li, L. Zhang, C. Hu, H. J. Jiang, J. D. Cao, Global Mittag-Leffler synchronization of fractional-order delayed quaternion-valued neural networks: Direct quaternion approach, *Appl. Math. Comput.*, **373** (2020), 125020. https://doi.org/10.1016/j.amc.2019.125020
19. M. F. Zhu, B. X. Wang, Y. H. Wu, Dynamical bifurcation of large-scale-delayed fractional-order neural networks with hub structure and multiple rings, *IEEE Trans. Syst. Man Cybern.: Syst.*, **52** (2022), 1731–1743. https://doi.org/10.1109/tsmc.2020.3037094

20. M. Hymavathi, T. F. Ibrahim, M. S. Ali, G. Stamov, I. Stamova, B. A. Younis, et al., Synchronization of fractional-order neural networks with time delays and reaction-diffusion terms via pinning control, *Mathematics*, **10** (2022), 3916. https://doi.org/10.3390/math10203916
21. W. Y. Xu, J. D. Cao, M. Xiao, D. W. C. Ho, G. H. Wen, A new framework for analysis on stability and bifurcation in a class of neural networks with discrete and distributed delays, *IEEE Trans. Cybern.*, **45** (2015), 2224–2236. https://doi.org/10.1109/tcyb.2014.2367591
22. X. H. Tian, R. Xu, Hopf bifurcation analysis of a reaction-diffusion neural network with time delay in leakage terms and distributed delays, *Neural Process. Lett.*, **43** (2015), 173–193. https://doi.org/10.1007/s11063-015-9410-0
23. L. Wang, H. Y. Zhao, J. D. Cao, Synchronized bifurcation and stability in a ring of diffusively coupled neurons with time delay, *Neural Networks*, **75** (2016), 32–46. https://doi.org/10.1016/j.neunet.2015.11.012
24. J. Chen, M. Xiao, X. Q. Wu, Z. X. Wang, J. D. Cao, Spatiotemporal dynamics on a class of (n+1)-dimensional reactionÂ¨Cdiffusion neural networks with discrete delays and a conical structure, *Chaos Solitons Fractals*, **164** (2022), 112675. https://doi.org/10.1016/j.chaos.2022.112675
25. J. J. He, M. Xiao, J. Zhao, Z. X. Wang, Y. Yao, J. D. Cao, Tree-structured neural networks: Spatiotemporal dynamics and optimal control, *Neural Networks*, **164** (2023), 395–407. https://doi.org/10.1016/j.neunet.2023.04.039
26. Y. X. Lu, M. Xiao, J. L. Liang, J. Chen, J. X. Lin, Z. X. Wang, et al., Spatiotemporal evolution of large-scale bidirectional associative memory neural networks with diffusion and delays, *IEEE Trans. Syst. Man Cybern.: Syst.*, **54** (2024), 1388–1400. https://doi.org/10.1109/tsmc.2023.3326186
27. J. Chen, M. Xiao, Y. H. Wan, C. D. Huang, F. Y. Xu, Dynamical bifurcation for a class of large-scale fractional delayed neural networks with complex ring-hub structure and hybrid coupling, *IEEE Trans. Neural Networks Learn. Syst.*, **34** (2023), 2659–2669. https://doi.org/10.1109/tnnls.2021.3107330
28. Y. X. Lu, M. Xiao, J. J. He, Z. X. Wang, Stability and bifurcation exploration of delayed neural networks with radial-ring configuration and bidirectional coupling, *IEEE Trans. Neural Networks Learn. Syst.*, **35** (2024), 10326–10337. https://doi.org/10.1109/tnnls.2023.3240403
29. Y. X. Lu, M. Xiao, X. Q. Wu, H. R. Karimi, X. P. Xie, J. D. Cao, et al., Tipping prediction of a class of large-scale radial-ring neural networks, *Neural Networks*, **181** (2025), 106820. https://doi.org/10.1016/j.neunet.2024.106820
30. W. H. Li, X. B. Gao, R. X. Li, Dissipativity and synchronization control of fractional-order memristive neural networks with reaction-diffusion terms, *Math. Methods Appl. Sci.*, **42** (2019), 7494–7505. https://doi.org/10.1002/mma.5873
31. W. J. Sun, G. J. Ren, Y. G. Yu, X. D. Hai, Global synchronization of reaction-diffusion fractional-order memristive neural networks with time delay and unknown parameters, *Complexity*, **2020** (2020), 1–14. https://doi.org/10.1155/2020/4145826
32. J. Z. Lin, J. P. Li, R. Xu, Turing instability and pattern formation of a fractional Hopfield reaction-diffusion neural network with transmission delay, *Nonlinear Anal.-Model. Control*, **27** (2022), 1–18. https://doi.org/10.15388/namc.2022.27.27473

33. B. Y. Datsko, V. V. Gafiychuk, Chaotic dynamics in Bonhoffer–van der Pol fractional reaction–diffusion system, *Signal Process.*, **91** (2011), 452–460. https://doi.org/10.1016/j.sigpro.2010.04.004

34. B. Datsko, V. Gafiychuk, Oscillatory wave bifurcation and spatiotemporal patterns in fractional subhyperbolic reaction-diffusion systems, *Commun. Nonlinear Sci. Numer. Simul.*, **142** (2025), 108601. https://doi.org/10.1016/j.cnsns.2025.108601

35. B. Datsko, V. Gafiychuk, Complex spatio-temporal solutions in fractional reaction-diffusion systems near a bifurcation point, *Fract. Calc. Appl. Anal.*, **21** (2018), 237–253. https://doi.org/10.1515/fca-2018-0015

36. Z. H. Wu, Z. M. Wang, Y. L. Cai, W. M. Wang, Turing pattern formation in a fractional-order reaction-diffusion Holling-IV predator-prey model, *Adv. Contin. Discrete Models*, **2025** (2025). https://doi.org/10.1186/s13662-025-03998-6

37. Y. H. Wu, M. K. Ni, Existence of traveling pulses for a diffusive prey¨Cpredator model with strong Allee effect and weak distributed delay, *Commun. Nonlinear Sci. Numer. Simul.*, **143** (2025), 108596. https://doi.org/10.1016/j.cnsns.2025.108596

38. I. Podlubny, *Fractional Differential Equations*, Academic Press, San Diego, California, 1999.

39. O. Brandibur, E. Kaslik, Stability of two-component incommensurate fractional-order systems and applications to the investigation of a FitzHugh-Nagumo neuronal model, *Math. Methods Appl. Sci.*, **41** (2018), 7182–7194. https://doi.org/10.1002/mma.4768

40. S. H. Liu, C. D. Wang, H. N. Wang, Y. H. Jing, J. D. Cao, Dynamical detections of a fractional-order neural network with leakage, discrete and distributed delays, *Eur. Phys. J. Plus*, **138** (2023), 575. https://doi.org/10.1140/epjp/s13360-023-04060-8

AIMS Press